



**SEVENTH FRAMEWORK
PROGRAMME
THEME [ENV.2010.2.1.5-1]
[Assessing vulnerability of urban systems, populations and goods in relation to
natural and man-made disasters in Africa]**

Grant agreement no: **265137**
Project acronym: **CLUVA**
Project title: "**CLimate change and Urban Vulnerability in Africa**"

Deliverable reference number and title: D2.1 Identification of hot spots vulnerability of
adobe houses, sewer systems and road networks

Due date of deliverable: 30/11/2012
Actual submission date: 04/06/2013

Start date of project: 01/12/2010

Duration: 36 months

Organisation name of lead contractor for this deliverable: AMRA – ANALISI E
MONITORAGGIO DEL RISCHIO AMBIENTALE SCARL

Revision [1]

Project co-funded by the European Commission within the Seventh Framework Programme (2007-2013)		
Dissemination Level		
PU	Public	X
PP	Restricted to other programme participants (including the Commission Services)	
RE	Restricted to a group specified by the consortium (including the Commission Services)	
CO	Confidential, only for members of the consortium (including the Commission Services)	



Note about contributors

The following organisations contributed to the work described in this deliverable:

Lead partner responsible for the deliverable:

[AMRA]

Deliverable prepared by: Raffaele De Risi, Fatemeh Jalayer

Partner responsible for quality control:

[KU]

Deliverable reviewed by:
Gertrud Jørgensen

Other contributors:

Name of contributor(s)

[AMRA]

Raffaele De Risi,
Fatemeh Jalayer
Francesco De paola
Maria Elena Topa
Iunio Iervolino
Maurizio Giugni

[EiABC]

Nebyou Yonas
Alemu Nebebe
Kumelachew Yeshitela

[ARDHI]

Deusdedit Kibassa
Riziki Shemdoe

[UM]

Gina Cavan
Sarah Lindley

[TUM]

Andreas Printz
Florian Renner



SUMMARY

Identifying the urban hot spots to flooding is one of the first steps in an integrated methodology for urban flood risk assessment and mitigation. This deliverable employs two GIS-based frameworks for identifying the urban hot spots for residential buildings and urban corridors. This is done by overlaying the map of potentially flood prone areas (the topographic wetness index, TWI, CLUVA Deliverable **D1.2**) and the map of urban morphology types (UMT, CLUVA Deliverable **D2.7**) classified as residential or as urban corridors. A maximum likelihood method (MLE) is employed for estimating the threshold used for identifying the flood-prone areas (the TWI threshold) based on the inundation profiles calculated for various return periods within a given spatial window. Furthermore, Bayesian parameter estimation is employed in order to estimate the TWI threshold based on inundation profiles calculated for more than one spatial window. For different statistics of TWI threshold (e.g., MLE estimate, 16th percentile, 50th percentile), the map of the flood prone areas is overlaid with the map of urban morphology units identified as residential and urban corridors in order to delineate the urban hot spots for both urban morphology types. Moreover, information related to population density is integrated by overlaying geo-spatial datasets created based on census data in order to estimate the number of people affected by flooding. Differences in exposure characteristics have been assessed for a range of different residential types. As a demonstration, the urban hotspots to flooding are delineated for different percentiles of the TWI value for the CLUVA case study cities of Addis Ababa, Dar es Salaam and Ouagadougou.

DISCLAIMER

This deliverable has been re-focused from its original title. The first instance regards a change of focus in order to discuss residential buildings in general and not only adobe houses. Another instance regards an extension of the focus in order to delineate the hot spots in term of flood hazard and not only in terms of flood vulnerability. The last instance regards the sewer systems which have not been addressed in this deliverable. Nevertheless, the procedure described later for the identification of urban hot spots can be also employed to the sewer systems.

The results presented for the case-study in Ouagadougou consist of the identification of urban flood hot spots in terms of hazard without considering information on exposure. This is due to lack of exposure data (e.g., Urban Morphology Types and population density datasets) for Ouagadougou at the time of the elaborations.

CONTENTS

1	INTRODUCTION	7
2	CONCEPTS AND METHODOLOGY	9
2.1	GIS-BASED IDENTIFICATION OF URBAN HOTSPOTS.....	9
2.1.1	<i>Delineation of flood-prone areas using the topographic wetness index (TWI)</i>	9
2.1.2	<i>Using the inundation profiles for the calibration of the TWI threshold</i>	10
2.1.3	<i>Delineation of geographical functional units using the Urban Morphology Types (UMT).....</i>	10
2.1.4	<i>Identification of urban hotspots by overlaying the TWI and UMT datasets</i>	11
2.2	MAXIMUM LIKELIHOOD ESTIMATION OF THE TWI THRESHOLD	12
2.2.1	<i>Estimation of the likelihood function using the areal extents.</i>	13
3	IDENTIFICATION OF URBAN HOT SPOTS.....	17
3.1	The case of Addis Ababa	17
3.1.1	<i>Delineation of flood-prone areas for Addis Ababa using the topographic wetness index (TWI).....</i>	18
3.1.2	<i>The inundation profile for Little Akaki</i>	18
3.1.3	<i>Maximum likelihood estimation of the flood-prone threshold</i>	20
3.1.4	<i>Using Bayesian parameter estimation in order to estimate τ based on information from more than one spatial window</i>	24
3.1.5	<i>UMT for Addis Ababa city</i>	26
3.1.6	<i>Identification of urban hotspots by overlaying the TWI and UMT datasets</i>	26
3.2	The case of Dar Es Salaam.....	31
3.2.1	<i>Delineation of flood-prone areas for Dar Es Salaam using the topographic wetness index (TWI).....</i>	31
3.2.2	<i>The inundation profile for Suna</i>	32
3.2.3	<i>Maximum likelihood estimation of the flood-prone threshold</i>	34
3.2.4	<i>UMT for Dar es Salaam</i>	38
3.2.5	<i>Identification of urban hotspots by overlaying the TWI and UMT datasets</i>	38
3.3	The case of Ougadougou.....	43
3.3.1	<i>Delineation of flood-prone areas for Ouagadougou using the topographic wetness index (TWI).....</i>	44
3.3.2	<i>The inundation profile</i>	45
3.3.3	<i>Maximum likelihood estimation of the flood-prone threshold</i>	46

List of figures

Figure 1- Hazard (H), Vulnerability (V) and Risk (R), the concept of an urban hot-spot.....	7
Figure 2 - The main components of the TWI calculation.	9
Figure 3 - Mapping UMT units using orthorectified aerial photography, an example in Addis Ababa.	11
Figure 4 - FP and IN areas.....	12
Figure 5 - Identification of the total urban area (A_{urban}) and the flood prone urban area ($A_{\text{urban}}(\text{FP})$) for a given threshold	14
Figure 6 - DEM of Addis Ababa (overlying the main water courses).....	17
Figure 7 - TWI for Addis Ababa	18
Figure 8 - Inundation profiles in terms of h_{max} [in meters] for various return periods for the case study area (Little Akaki)	19
Figure 9 - The TWI and the spatial the window for hydraulic analyses at Little Akaki.....	20
Figure 10 - a) Probability of being <i>FP</i> and <i>IN</i> given τ . b) Probability of being \overline{FP} and \overline{IN} given τ .	21
Figure 11 - a) The likelihood function $L(\tau W)$ (also the probability density for τ); b) threshold <i>CDF</i>	22
Figure 12 - Overlay of FP and IN areas for the spatial window <i>W</i> (Little Akaki).	22
Figure 13 - a) Zones 1 and 2. b) $p(\tau W_1)$:the posterior distribution calculated for the Zone1 and used as prior for Zone 2.....	24
Figure 14 - a) the likelihood $L(\tau W_2)$; b) the posterior distribution $p(\tau W_1, W_2)$	25
Figure 15 - High level UMT map for Addis Ababa.....	26
Figure 16 - The urban residential hot spots for flooding delineated for different TWI thresholds: a) residential area, b)16 th percentile, c) τ_{ML}^- , d)maximum likelihood, e) 50 th percentile, f) τ_{ML}^+	28
Figure 17 - Breakdown of the residential hot-spot in terms of flood prone residential area and people affected by flooding in the residential area.	29
Figure 18 - The urban corridor hot spots for flooding delineated for different TWI thresholds: a) residential area, b)16 th percentile, c) τ_{ML}^- , d)maximum likelihood, e) 50 th percentile, f) τ_{ML}^+	30
Figure 19 - a) Tanzania, b) Dar Es Salaam city.....	31
Figure 20 - TWI for Dar Es Salaam.....	32
Figure 21 - Inundation profiles in terms of h_{max} [in meters] for various return periods for the case study area.....	33
Figure 22 - The TWI and the spatial the window for hydraulic analyses at Suna.....	34
Figure 23 - a) Probability of being <i>FP</i> and <i>IN</i> given τ . b) Probability of being \overline{FP} and \overline{IN} given τ .	35
Figure 24 - a) The likelihood function $L(\tau W)$ (also the probability density for τ); b) threshold <i>CDF</i>	36
Figure 25 - Overlay of FP and IN areas for the spatial window <i>W</i>	36
Figure 26 - a) The likelihood function $L(\tau W)$. b) threshold <i>CDF</i> for different return periods.	37
Figure 27 - High level UMT map for Dar es Salaam.....	38
Figure 28 - The urban residential hot spots for flooding delineated for different TWI thresholds: a) residential area, b)16 th percentile, c) τ_{ML}^- , d)maximum likelihood, e) 50 th percentile, f) τ_{ML}^+	40



Figure 29 - Breakdown of the residential hot-spot in terms of flood prone residential area and people affected by flooding in the residential area.	41
Figure 30 - The urban corridor hot spots for flooding delineated for different TWI thresholds: a) residential area, b) 16 th percentile, c) τ_{ML}^- , d) maximum likelihood, e) 50 th percentile, f) τ_{ML}^+	42
Figure 31 - Burkina Faso, with Ouagadougou position (in red).....	44
Figure 32 - TWI for Ouagadougou	45
Figure 33 - Inundation profile of the event append in Sep 09.....	45
Figure 34 - a) Inundation areas after the 2009 events, b) Area 1 (the smaller) and Area 2 (the bigger)	46
Figure 35 - The likelihood function $L(\tau W_1, W_2)$, b) threshold CDF	46
Figure 36 - a) Matching for the inundate areas, b) flood prone areas for the entire city	47

List of Tables

Table 1 - The statistics for the TWI threshold distribution as a function of the return period.....	23
Table 2 - Exposure to flooding risk in terms of the estimated percent of residential area and people affected by flooding	28
Table 3 - Exposure assessment in terms of urban corridors.....	30
Table 4 - The statistics for the TWI threshold distribution as a function of the return period.....	37
Table 5 - Exposure to flooding risk in terms of the estimated percent of residential area and people affected by flooding	40
Table 6 - Exposure assessment in terms of urban corridors.....	42
Table 7 - The statistics for the TWI threshold distribution for the case of Ouagadougou.....	47

1 INTRODUCTION

The hot spots in an urban setting can be defined as the zones likely to be exposed to climate-related extreme events such as flooding. Arguably, identifying the urban hot spots to flooding is one of the first steps in an integrated methodology for urban planning and risk management. The delineation of urban hotspots not only can provide useful information for the policy makers but also it can be useful as support information for indicating future urban dynamics and trends. Figure 1 illustrates a schematic representation of an urban hot spot identified as R (standing for risk) as an area in which high probability of occurrence of climate related events identified as H (standing for hazard) coincides with areas of high vulnerability identified as V (e.g., vulnerable buildings, vulnerable roads, ..., etc.).

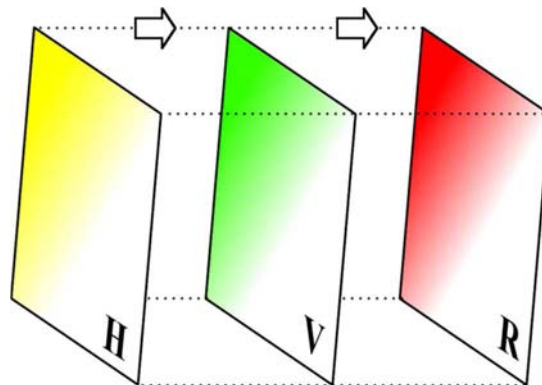


Figure 1- Hazard (H), Vulnerability (V) and Risk (R), the concept of an urban hot-spot.

This work employs two GIS-based frameworks for identifying the urban hot spots for residential buildings and urban corridors (i.e., major roads). This is done by overlaying a map of potentially flood prone areas (identified by the topographic wetness index, TWI) and a map of urban morphology types (UMT) classified as residential or as urban corridors. The topographic wetness index (TWI, [Qin et al. 2011](#)) allows for the delineation of a portion of a hydrographic basin potentially exposed to flood inundation by identifying all the areas characterized by a topographic index that exceed a given threshold. The urban morphological types ([Pauleit and Duhme 2000](#), [Gill et al. 2008](#), [Cavan et al. 2012](#)) form the foundation of a classification scheme which brings together facets of urban form and function. The application of the UMTs allows the delineation of geographical units. The distinction of UMTs at a ‘meso’-scale (i.e. between the city level and that of the individual units) makes a suitable basis for the spatial analysis of cities.

The TWI threshold value depends on the resolution of the digital elevation model (DEM), topology of the hydrographic basin (i.e. urban, peri-urban or rural) and the constructed infrastructure ([Manfreda et al. 2008, 2011](#)). Assuming that the urban territory can be characterized by a single threshold value, one can calibrate this threshold based on the results of detailed delineation of the inundation profile for selected zones. In this study, the TWI threshold is calibrated based on the calculated inundation profiles for various return periods for selected zones within the basin through a Bayesian framework. The Bayesian framework enables the probabilistic characterization of the threshold by calculating the complementary probability of false delineation of flood prone zones as a function of various threshold values. For a given return period, the probability of false delineation



is calculated as the sum of the probability of indicating a zone flood prone, while it is not indicated as such by the inundation profile, and the probability that a zone is indicated as not flood prone but indicated as flood prone by the inundation profile. Applying the above-mentioned procedure, taking into account all available information on the inundation profiles for various zones within the basin, leads to a probability distribution for the TWI threshold value.

In the next step, the urban residential hot spots to flooding are delineated in the GIS environment by overlaying the map of TWI and the UMT units classified as residential for various percentiles of the TWI threshold. Additional information related to exposure such as population density and demographic information can be integrated by overlaying geo-spatial datasets created based on census data. Differences in exposure characteristics can be assessed for a range of different residential types, including for example between condominium/multi-storey, single storey stone/concrete and areas predominantly associated with mud/wood construction. For each percentile value considered, the delineated flood-prone residential areas and the number of people potentially affected to flooding are calculated. Moreover, the potential dependence of the estimated threshold percentiles on the flooding return period is investigated. As a demonstration, the urban residential hotspots to flooding are delineated for different percentiles of the TWI value for the cities of Addis Ababa (Ethiopia) and Dar Es Salaam (Tanzania). Moreover, the TWI threshold values are calibrated for the city of Ouagadougou (Burkina Faso) based on the observed spatial extent of the 2009 flooding event in the city.

2 CONCEPTS AND METHODOLOGY

2.1 GIS-BASED IDENTIFICATION OF URBAN HOTSPOTS

2.1.1 Delineation of flood-prone areas using the topographic wetness index (TWI)

The topographic wetness index, initially introduced by Kirkby (1975), has been shown to be strongly correlated to the area exposed to flood inundation (Manfreda et al. 2007; 2008; 2011). The TWI for a given point O within the hydrographic basin is calculated as following:

$$TWI = \log \left(\frac{A_s}{\tan \beta} \right) \quad (1)$$

where A_s is the specific catchment area expressed in meters and calculated as the local up-slope area draining through point O per unit contour length (A/L); β is the local slope at the point in question expressed in degrees. Figure 2 illustrates the main components used for the calculation of the TWI at a given point O within the hydrographic basin, namely the catchment area A for point O , the length L of the contour line, and the specific catchment area A_s .

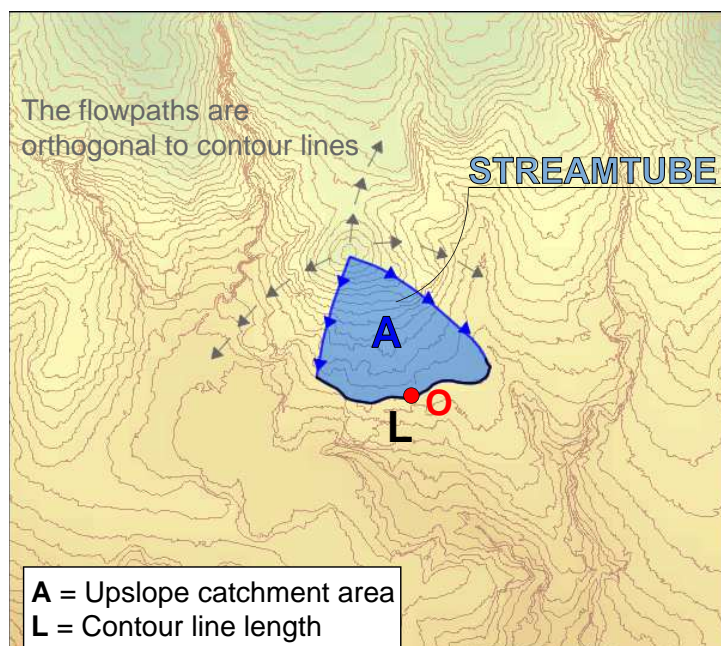


Figure 2 - The main components of the TWI calculation.

The TWI allows for the delineation of a portion of a hydrographic basin potentially exposed to flood inundation (referred to herein as flood prone or more briefly as FP) by identifying all the areas characterized by a topographic index that exceeds a given threshold. The TWI threshold value depends on the resolution of the digital elevation model (DEM), the topology of the hydrographic basin (i.e. urban, per-urban or rural) and the presence of constructed infrastructures (e.g. sewage system, bridges, culverts, ..., etc.). This threshold is usually calibrated based on the results of detailed delineation of the inundation profile for selected zones.

Data quality:

The TWI is strictly related to the DEM quality. A good practice for ensuring a high-resolution TWI map is to use DEM with horizontal and vertical resolution between 1 to 2 meters.

2.1.2 Using the inundation profiles for the calibration of the TWI threshold

As it was mentioned in the previous section, the TWI method delineates the flood prone areas as the portions of the basin for which the topographic index exceeds a prescribed threshold. One way for establishing the TWI threshold is to use the available inundation profile for one (or more) zones of interest within the basin. The inundation profile, reported as the flooding heights (and velocities) for various nodes within a lattice covering a given area for different return periods, can be obtained by means of classic hydraulic routines of various degrees of sophistication and accuracy (Apel et al. 2009). The calculation of the inundation profiles can be summarized in a step-by-step manner as follows:

1. The definition of the rainfall curves for different return periods (T_R) based on historic rainfall annual maxima.
2. The acquisition of cartographic information such as, digital elevation model (DEM), digital surface model (DSM), the geology map, and the land-use map, for the zone(s) of interest.
3. Calculation of the hydrographs for the various return periods associated to the rainfall curves. The hydrograph refers to the flow discharge as a function of time and constitutes the input for the hydraulic diffusion model. The area under the hydrograph is equal to the total discharge volume for the basin under study.
4. Diffusion of the total discharge volume (area under the hydrograph) based on the general constitutive equations of continuity and fluid dynamics (i.e. one-dimensional or bi-dimensional diffusion models). This can be done by means of various software tools (e.g., FLO2D, 2004; HEC-RAS, 2010; ..., etc.).

The inundation profile, obtained through a procedure similar to the one described above, can be used to delineate the inundated areas (referred to herein as IN), for a given return period, as those areas within the zones of interest where the inundation height is greater than zero.

2.1.3 Delineation of geographical functional units using the Urban Morphology Types (UMT)

The urban morphology types UMT form the foundation of a classification scheme which brings together facets of urban form and function. The UMT's can be viewed as a geo-spatial dataset, containing seamless polygons of each *UMT unit*, which include specific information for each land parcel within an associated attribute table, such as, the UMT code, geometric properties, etc. This geospatial layer provides complete and consistent coverage across the city. Therefore, internal consistency in data recording and coding in attribute tables is essential in the process of delineation of the UMT units. Linear features such as roads and rivers can be used as the outline of UMT units, and matched with administrative units/zones where possible, e.g. for the boundary of the dataset, as shown in Figure 3.

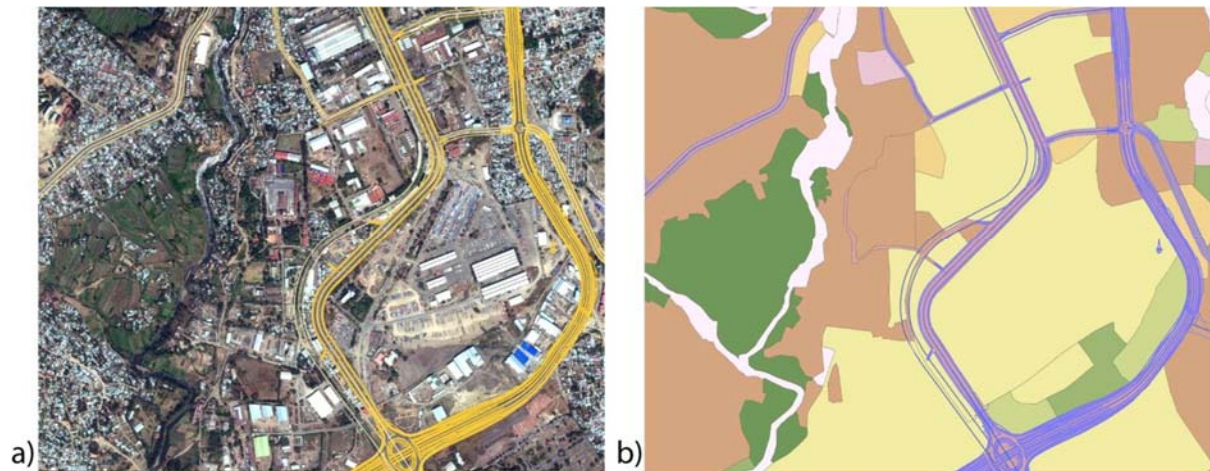


Figure 3 - Mapping UMT units using orthorectified aerial photography, an example in Addis Ababa.

In order to build a UMT map, it is necessary to identify the various *UMT classes* for the specific urban area (e.g., farmland, transport, residential, etc.). The UMT classes can be detected through visual analysis of remote sensing data (ortho-rectified aerial photography) as the primary method of applying the scheme (Gill et al. 2008). Furthermore, for each UMT class, typical images can be captured and kept for reference with a description of its characteristics. Finally the maps should be checked through field trips and eventually revised where necessary. Once a complete UMT layer has been created through the process of digitisation, it is then suitable for further GIS analysis, and can be combined with other datasets to produce spatial indicators.

2.1.4 Identification of urban hotspots by overlaying the TWI and UMT datasets

In this work, the urban hotspots for residential areas and major urban corridors are identified by overlaying the layer of flood prone areas identified by TWI values larger than the threshold τ and the layers delineating the urban morphology units identified as residential and major urban corridor types, respectively. In the following section, a probabilistic method for estimating the TWI threshold is presented. Therefore, the urban hotspots are identified taking into account not just a single value of the TWI threshold but considering its probability distribution. Obviously, considering the probability distribution for τ (in other words, the uncertainty in the evaluation of τ), is going to influence the results in terms of the spatial extent of the hot spots and the estimated number of people affected.

2.2 MAXIMUM LIKELIHOOD ESTIMATION OF THE TWI THRESHOLD

The delineation of flood-prone areas is strictly dependent on the TWI threshold, assuming that the urban territory can be characterized by a single threshold value. In this study, the TWI threshold is calibrated probabilistically based on the calculated inundation profiles for various return periods for a selected zone within the basin by employing the maximum likelihood parameter estimation. This section describes how the likelihood function for the TWI threshold is calculated based on the inundation profile available for a selected (micro-scale) zone of interest within the basin.

Let W represent the spatial window of a zone of interest (within the basin) for which the inundation profile is calculated. Moreover, let FP represent the flood-prone areas identified as $TWI > \tau$ and $IN(T_R)$ represent the inundated areas for a given return period T_R identified as $h(T_R) > 0$; where $h(T_R)$ is the flooding height calculated for a given point within the zone of interest W . Figure 4(a) illustrates in a schematic manner zone W and the portions identified as FP and $IN(T_R)$.

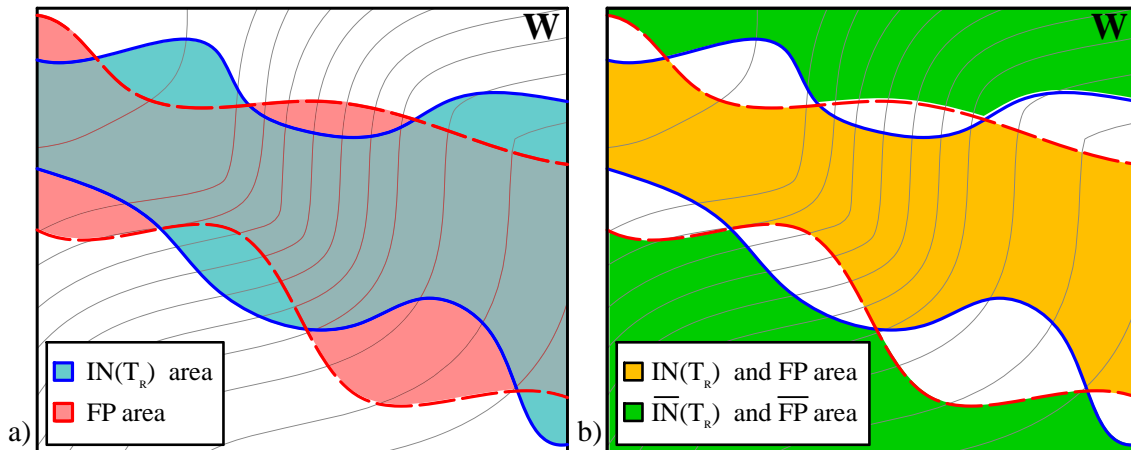


Figure 4 - Schematic diagrams of the spatial window W : (a) the areas indicated as flood prone by the TWI (FP) and the inundation profiles ($IN(T_R)$) (b) the intersection of the areas indicated as flood prone by TWI and the inundation profile; and the intersection of the areas indicated as NOT flood-prone by TWI and the inundation profiles.

Let W represent the spatial window of a zone of interest (within the basin) for which the inundation profile is calculated. Moreover, let FP represent the flood-prone areas identified as $TWI > \tau$ and $IN(T_R)$ represent the inundated areas for a given return period T_R identified as $h(T_R) > 0$; where $h(T_R)$ is the flooding height calculated for a given point within the zone of interest W . Figure 4 (a) illustrates in a schematic manner zone W and the portions identified as FP and $IN(T_R)$.

The probability of the correct delineation of the flood-prone areas or the likelihood function for the TWI threshold τ denoted as $L(\tau|W)$ for various values of τ can be calculated as following:

$$L(\tau|W) = P(FP, IN(T_R) | \tau, W) + P(\overline{FP}, \overline{IN(T_R)} | \tau, W) \quad (2)$$

where $P(FP, IN(T_R) | \tau, W)$ denotes the probability that a given point within zone W is identified both as flood-prone FP (using the TWI method) and inundated $IN(T_R)$ (using the more accurate

inundated profiles), for a given return period T_R and conditioned on (the | sign) a given value of τ of the TWI threshold. The area FP and $IN(T_R)$ is indicated by colour orange in Figure 4(b). Similarly, $P(\overline{FP}, \overline{IN(T_R)} | \tau, W)$ denotes the probability that a given point within the zone of interest is neither identified as FP nor as $IN(T_R)$ conditioned on a given value of τ of the TWI threshold. The area not FP and not $IN(T_R)$ is indicated by colour green in Figure 4(b). It can be shown that the likelihood function in Eq. 2 can be equivalently expressed as the complement of probability of false delineation of flood-prone areas or the so-called *cry-wolf*:

$$L(\tau|W) = 1 - P(\overline{FP}, \overline{IN(T_R)} | \tau, W) - P(\overline{FP}, IN(T_R) | \tau, W) \quad (3)$$

where $P(\overline{FP}, \overline{IN(T_R)} | \tau, W)$ for a given point within zone W denotes the probability that it is indicated as FP by the TWI method but not $IN(T_R)$ in the more accurate delineation of the inundated zones. Vice versa, $P(\overline{FP}, IN(T_R) | \tau, W)$ for a given point within zone W denotes the probability that it is not indicated as FP but its results as inundated in the delineation of the inundated zones.

Going back to Eq. 2, the terms $P(FP, IN | \tau, W)$ and $P(\overline{FP}, \overline{IN} | \tau, W)$ can be expanded, using the probability theory's product rule (Jaynes, 1995), as following:

$$P(FP, IN(T_R) | \tau, W) = P(FP | \tau, W) \cdot P(IN(T_R) | FP, \tau, W) \quad (4)$$

$$P(\overline{FP}, \overline{IN(T_R)} | \tau, W) = P(\overline{FP} | \tau, W) \cdot P(\overline{IN(T_R)} | \overline{FP}, \tau, W) \quad (5)$$

where the term $P(IN | FP, \tau, W)$ for a given point denotes the probability of being IN given that it is identified as FP and $P(\overline{IN} | \overline{FP}, \tau, W)$ denotes the probability of not being IN conditioned on not being FP, given the threshold value τ . The terms $P(FP | \tau, W)$ and $P(\overline{FP} | \tau, W)$ represent the probability of being FP or not being FP respectively, given the TWI threshold value τ .

2.2.1 Estimation of the likelihood function using the areal extents

Part 1-The micro-scale estimations: Let $A_w(FP)$ denote the areal extent of the flood-prone portion of the zone W identified via the TWI method (note that $A_w(FP)$ is a function of τ since the flood-prone areas are identified as areas with $TWI > \tau$, the extent of the portion coloured as red in Figure 4(a)) and $A_w(IN(T_R))$ the areal extent of the inundated portion of W identified via hydraulic calculations for a given return period (the extent of the portion coloured as blue in Figure 4(a)). Analogously, $A_w(\overline{FP})$ and $A_w(\overline{IN(T_R)})$ refer to the areas of the not flood-prone and not inundated portions, respectively. The probability terms $P(IN(T_R) | FP, \tau, W)$ and $P(\overline{IN(T_R)} | \overline{FP}, \tau, W)$ can be estimated by the ratio of areal extents, as expressed in the following:

$$P(IN(T_R) | FP, \tau, W) = \frac{A_w(IN(T_R), FP)}{A_w(FP)} \quad (6)$$

$$P(\overline{IN(T_R)} | \overline{FP}, \tau, W) = \frac{A_W(\overline{IN(T_R)}, \overline{FP})}{A_W(\overline{FP})} \quad (7)$$

where $A_W(IN(T_R), FP)$ denotes the areal extent of the portion of the area W that is both FP and $IN(T_R)$ (the extent of the area coloured as orange in Figure 4(b)); $A_W(\overline{IN(T_R)}, \overline{FP})$ denotes the areal extent of the portion of the area W that is neither FP nor $IN(T_R)$ (the extent of the area coloured as green in Figure 4(b)). As mentioned above, the areal extents $A_W(IN(T_R), FP)$, $A_W(\overline{IN(T_R)}, \overline{FP})$, $A_W(FP)$ and $A_W(\overline{FP})$ are --by definition-- all functions of the TWI threshold τ .

Part 2-The meso-scale estimations: In the previous section, it was demonstrated how $P(IN(T_R) | FP, \tau, W)$ and $P(\overline{IN(T_R)} | \overline{FP}, \tau, W)$ were estimated using the areal extent ratios calculated in a micro-scale delineated by window W . However, also $P(FP | \tau, W)$ and $P(\overline{FP} | \tau, W)$ need to be estimated in order to be able to calculate the likelihood function. It has been chosen to estimate the above two terms using the areal extents calculated in the meso-scale (city-scale)¹. Denoting the total administrative area of the city under consideration as A_{urban} and denoting the total areal extent within the city having TWI greater than the given threshold τ as $A_{urban}(FP)$, one can estimate the term $P(FP | \tau)$ ² as:

$$P(FP | \tau) = \frac{A_{urban}(FP)}{A_{urban}} \quad (8)$$

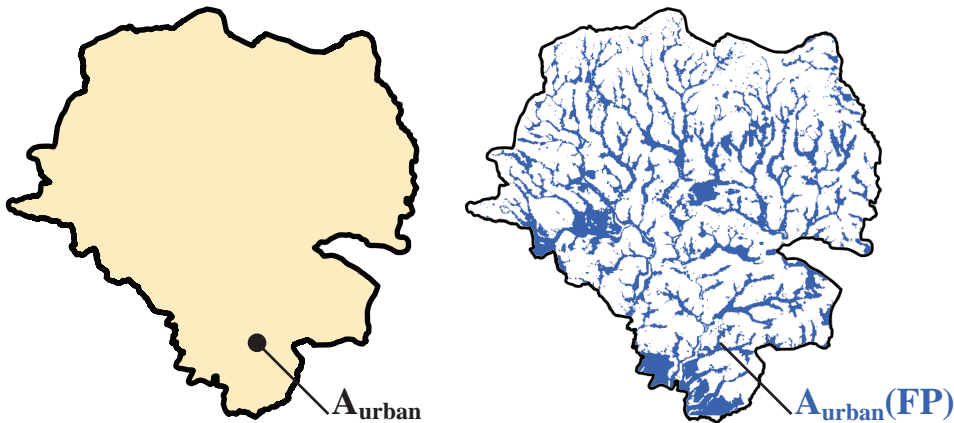


Figure 5 - Identification of the total urban area (A_{urban}) and the flood prone urban area ($A_{urban}(FP)$) for a given threshold

¹ Note that this term could have also been estimated based on the information contained within window W . However, it was chosen to use the whole extent of the city as reference. Therefore, in this case the information provided by the inundation profiles within W is not used. In fact, the term $P(FP | \tau, W)$ for simplicity is referred to as $P(FP | \tau)$ hereafter.

² The conditioning on W is left out for brevity and simplicity of formulations.

Figure 5 demonstrates schematically the areal extents A_{urban} and $A_{\text{urban}}(\text{FP})$ for a given value of τ for the city of Addis Ababa. The probability $P(\text{FP}|\tau)$ can then be calculated as $1 - P(\text{FP}|\tau)$.

Finally, the likelihood function in Eq. 2 can be calculated by substituting the terms calculated in Eqs. 6,7 and 8 in Eqs. 4 and 5 and summing up these two last equations. The maximum likelihood estimate for the TWI threshold can be calculated as the τ value that maximizes the likelihood function in Eq. 2.

Using Bayesian parameter estimation in order to estimate τ based on information from more than one spatial window

Suppose that some background information is available on the value of the TWI threshold τ . In that case, the maximum likelihood method presented in the previous section can be extended to a Bayesian parameter estimation, where the available background information is represented by a *prior* probability distribution. That is, the *posterior* probability distribution for τ given the information provided by the inundation profile within the spatial window W can be expressed as³:

$$p(\tau|W) = \frac{L(\tau|W)p(\tau)}{\sum L(\tau|W)p(\tau)} \quad (9)$$

where $p(\tau|W)$ denotes the posterior probability distribution for τ given spatial window W ; $L(\tau|W)$ is the likelihood function for τ calculated in the previous section and $p(\tau)$ is the prior probability distribution for τ before having the information on the inundation profile for window W . Note that Eq. 9 is particularly useful for calculating the threshold τ having the inundation profiles for than one spatial window within the basin. In that case, the posterior probability $p(\tau|W_1)$ can be used as prior probability distribution in order to calculate the posterior probability distribution $p(\tau|W_1, W_2)$ considering both spatial windows W_1 and W_2 and so on and so forth.

Calibration of TWI threshold based on information other than the inundation profile

It is worth noting that the probabilistic methodology presented in this report for the estimation of TWI threshold can also be used based on information other than the inundation profile. For instance, approximate maps delineating the flood prone areas for a city (e.g., based on historical information) can be used instead of the inundation profile for calibrating the threshold. Of course, in this case, the spatial window of interest W would be equal to the entire area of the city or the partial area for which the flood prone areas are delineated.

³ Strictly speaking, the formulation in Eq. 9 should have been conditioned on the "correct identification" of the flood-prone areas for window W (see Eq. 2). However, for the sake of simplicity and tractability of the equations, we have used the symbol W in order to imply in, a concise manner, all the additional information about the inundation profile contained within window W .

A simple description of the methodology adopted for the calibration of TWI threshold

The topographic wetness index (TWI) is used as a proxy for delineating the potentially flood-prone areas in the meso-scale. One of the most important components of the TWI map is the TWI threshold since the potentially flood-prone areas are identified as those with TWI greater than the threshold. In this deliverable, the TWI threshold is updated through a probabilistic method based on available information such as inundation profiles for various return periods or historical flooding data. How this calibration works? The first important step is to delineate the spatial window that contains the additional information that are going to contribute towards the calculation of the threshold. Then, the threshold is chosen as the value that maximizes the probability of the correct identification of the flood-prone areas based on the available additional information within window W . The probability of correct identification for a given threshold value can be calculated as the sum of two probability terms, namely, the probability that the TWI map and the additional information both indicate that the area within W is flood-prone and the probability that the TWI map and the additional information both indicate that the area within window W is not flood-prone. These probability terms are estimated as the ratio of areal extents. For example, the probability that both TWI and inundation maps indicate that the area is flood prone is first expanded as the product of the probability that the area is flood-prone based on the inundation profile given that it is flood-prone also based on the TWI and the probability that area is flood-prone based on TWI. The former term can be estimated as the ratio of the extent of area that is identified as flood-prone within W by the inundation profile clipped over the area that is indicated as flood prone by TWI, divided by the total areal extent identified as flood prone by TWI. The estimation of probability terms as ratio of areal extents renders the procedure particularly suitable for GIS-based implementations. Finally, the TWI threshold that is calibrated based on information available within W is going to be used in order to create the map of potentially flood-prone areas in the meso-scale.

3 IDENTIFICATION OF URBAN HOT SPOTS

In the following, the methodology described in the previous section is applied to two CLUVA case study cities: Addis Ababa and Dar Es Salaam. For both the cities, the calibration of the TWI threshold is realized based on calculated inundation profiles.

3.1 THE CASE OF ADDIS ABABA

In the following, the methodology described earlier is implemented in order to identify the urban hot spots for residential buildings and major urban corridors for flooding phenomenon in the city of Addis Ababa (for brevity referred to also as Addis), Ethiopia. Addis is the capital and the largest city in Ethiopia, with a population of 2739551 according to the 2007 population census⁴. The city is situated in the high plateaus of central Ethiopia in the North-South oriented mountain systems neighbouring the Rift-Valley. The city is overlooked by the mount Yarer in the east, the mount Entoto in the north and the mount Wochecha in the west part. The orography of Addis Ababa is represented in Figure 6 by a digital elevation model (DEM), overlaying also the main water courses in the city.

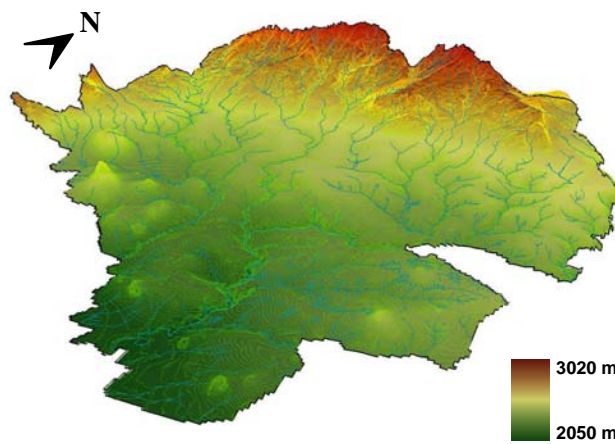


Figure 6 - DEM of Addis Ababa (overlying the main water courses)

Several small streams originate in the mountains surrounding the city and flow into the metropolitan area of Addis Ababa. Torrential rains, which are common during the rainy season, cause sudden rise in the flow of these streams and periodically inundate the settlements built along their banks.

The flooding of August 2006, the worst in Ethiopian history, has affected 363000 people and has left approximately 200000 people homeless. The maximum rainfall in the month of July 2006, prior to the catastrophic event, reached the record value of 245 mm. The final death toll is estimated at around 647. Lifelines were affected across the country. For instance, the telephone and power lines were interrupted and the main roads to Addis Ababa were blocked rendering the city inaccessible.

⁴ It is worth mentioning that the population of Addis is growing very fast. The precise figure reported above is the reference total population in the population density dataset used herein.

Last but not least, the floods have had a severe impact on urban agriculture, leading to widespread food shortages in one of the world's poorest states.

3.1.1 Delineation of flood-prone areas for Addis Ababa using the topographic wetness index (TWI)

The topographic wetness index is calculated in the GIS framework by applying Eq. 1 and based on the digital elevation model of the city (vertical resolution: 1 meters). Figura 7 illustrates the resulting TWI map for Addis. It can be observed that the TWI values vary between 7 and 22; in particular, largest TWI values can be spotted around the natural water channels.

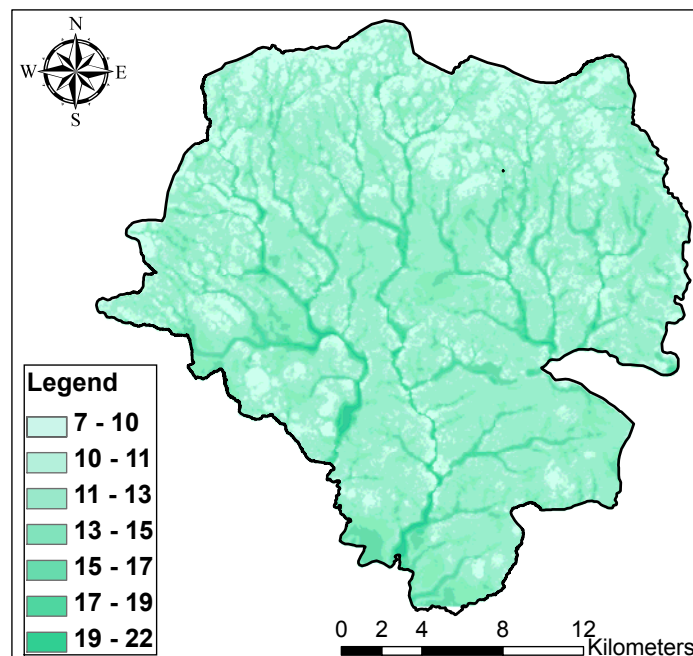


Figura 7 - TWI map for Addis Ababa

3.1.2 The inundation profile for Little Akaki

In order to calibrate the TWI threshold for Addis, the inundation profile for various return periods have been calculated for the Little Akaki area located in the southern part of Addis. Little Akaki results as flood-prone based on past flooding experiences. The inundation profile has been calculated by bi-dimensional simulation of flood volume propagation using the software FLO2D (using historical rainfall records, the DEM, and the calculation of the hydrograph based on the curve number method) assuming a simulation time of 45 hours. The outcome of the flood propagation is illustrated in Figure 8 in terms of maximum flow depth h_{max} with reference to five considered return periods (T_R 10, 30, 50, 100 and 300 years).

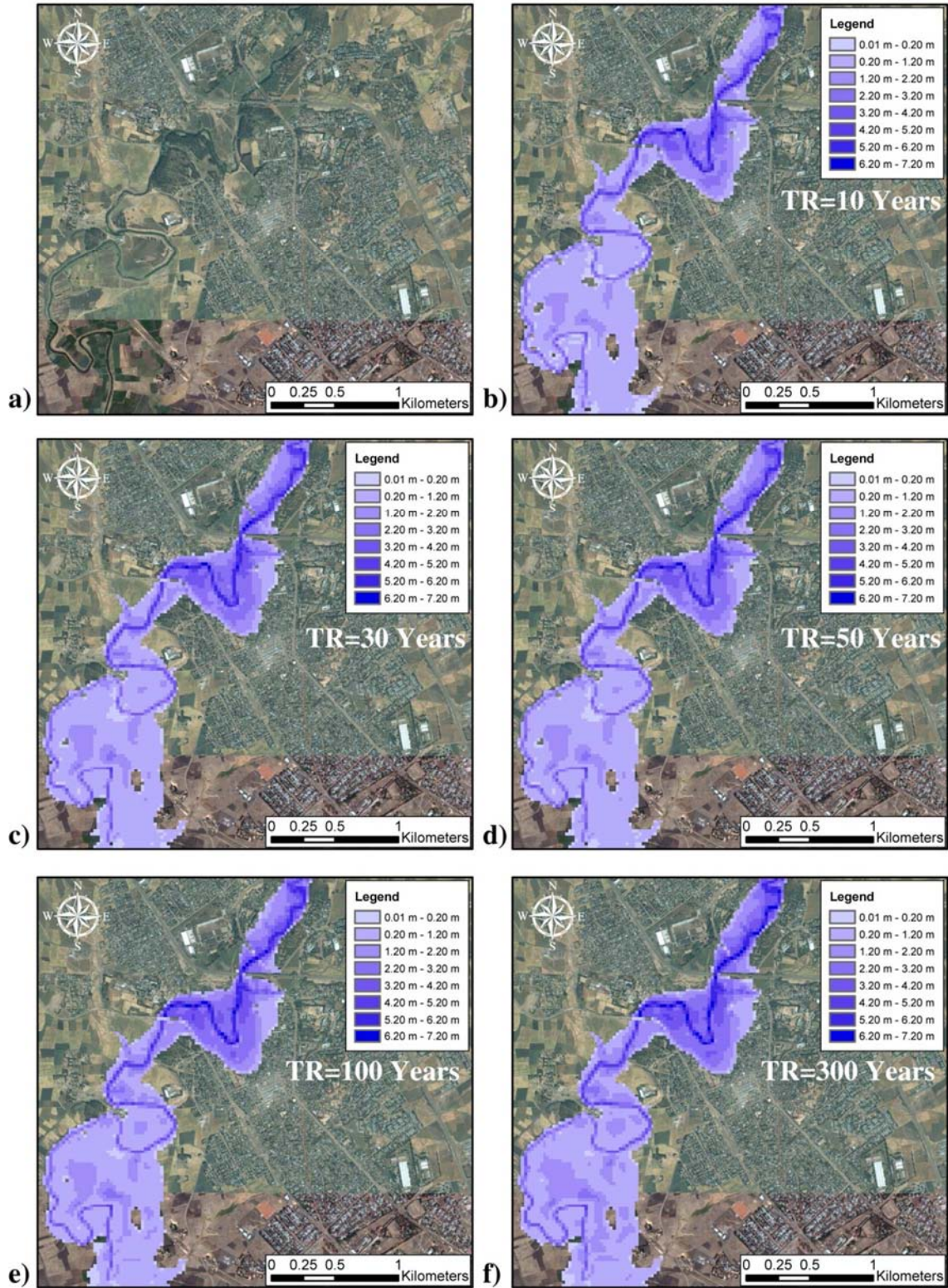


Figure 8 - Inundation profiles in terms of h_{max} [in meters] for various return periods for the case study area (Little Akaki)

3.1.3 Maximum likelihood estimation of the flood-prone threshold

In this section, it is demonstrated how the procedure described previously in the methodology can be applied in order to calculate the likelihood of being flood prone as a function of the TWI threshold.

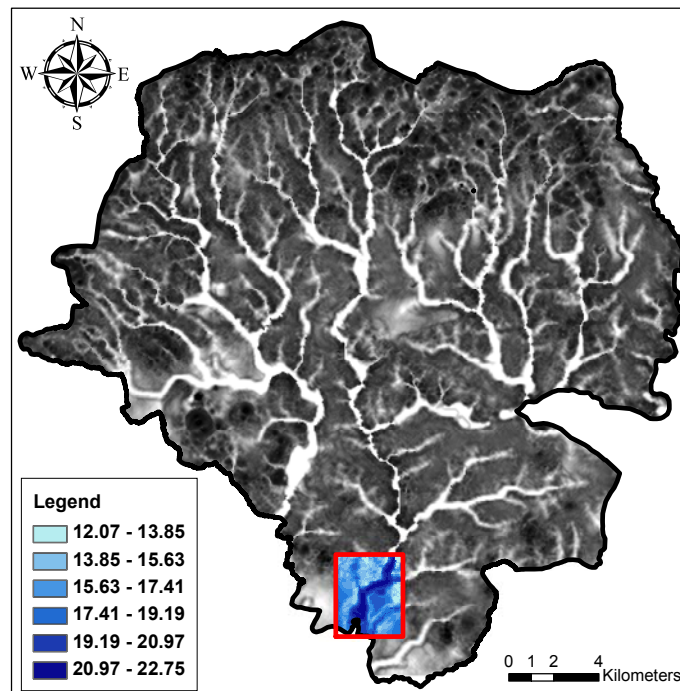


Figure 9 - The TWI and the spatial window for hydraulic analyses in Little Akaki

A spatial window identified as W with $A(W)$ around 11 km^2 is defined in the zone of little Akaki (Figure 9). For a return period $T_R=100$ years and for all the possible values of τ , the probability that a given zone is flood prone $P(\text{FP}|\tau)$ is calculated from Eq. 8 (based on meso-scale estimations) and is plotted in Figure 10(a) (as the black dots). Moreover, the probability that a given point is inundated $P(\text{IN}|\text{FP}, \tau)$ given that it is already indicated as FP for a given value of τ is calculated from Eq. 6 (based on micro-scale estimations) and plotted in Figure 10(a) (as the stars in gray). The probability that a given point is indicated both as flood prone (by the TWI method) and inundated (based on the hydraulic profile), $P(\text{FP}, \text{IN}|\tau)$ is calculated from Eq. 4 as the product of $P(\text{FP}|\tau)$ and $P(\text{IN}|\text{FP}, \tau)$ from Eq. 4 and plotted in Figure 10 (a) (as the circles in red). In a similar manner, the probability that a given point is not indicated as flood prone based on the TWI method is calculated as the complementary probability of being flood prone in Eq. 8 and plotted in Figure 10(b) (as the black dots). The probability that a given zone is not indicated as inundated given that it is not flood prone for a given value of τ is calculated from Eq. 7 and is plotted as the gray stars in Figure 10(b). Finally the probability that a given point is not inundated and not flood prone for a given value of τ , is calculated from Eq. 5 and plotted as the red circles in Figure 10(b).

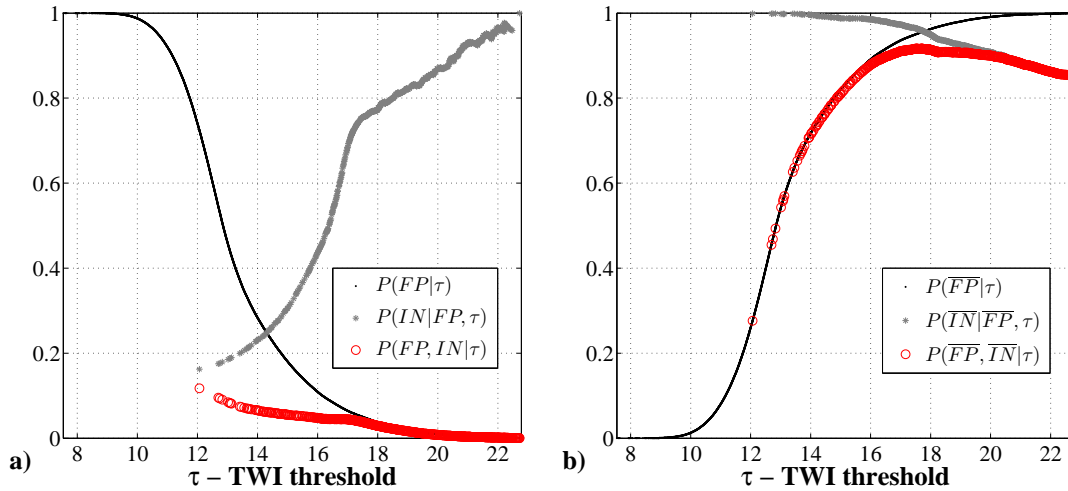


Figure 10 - a) Probability of that the area within the spatial window is indicated as flood prone by both TWI and inundation maps (FP and IN) given threshold value τ b) Probability that the area within the spatial window is indicated as not flood prone by both TWI and inundation maps (\overline{FP} and \overline{IN}) given threshold value τ

The likelihood function for window W at $T_R=100$ years is finally calculated from Eq. 2 by summing up the probability of being flood prone and inundated and the probability of not being flood prone and not being inundated for all possible τ values (i.e., summing up the curves illustrated by red circles in Figure 10(a) and Figure 10(b)). It is noteworthy that the probability $P(FP|\tau)$ and its complement are both defined in the domain of the threshold values ranging between 7.5 and 22.8 (the meso-scale estimations, Figura 7). Instead, the terms $P(IN|FP, \tau)$ and $P(\overline{IN}|\overline{FP}, \tau)$ are defined in the domain ranging between 12.07 and 22.78 (the micro-scale estimations, Figure 9).

The resulting likelihood function $L(\tau|W)$ is plotted in Figure 11(a) as a function of the TWI threshold τ . Consequently, the maximum likelihood estimate for τ (i.e., the value that corresponds to the maximum likelihood) can be identified as $\tau=17.11$. Furthermore, by identifying the τ values corresponding to 99% of the maximum likelihood value, it is possible to define a maximum likelihood interval, that varies between $\tau_{ML}^- = 16.66$ and $\tau_{ML}^+ = 17.89$. That is, from a practical point of view, the information used for calibrating the TWI threshold lead to identifying a maximum likelihood interval [16.66, 17.89] for τ .

Recalling that the likelihood function also represents the probability density function (PDF) for τ , the cumulative distribution for τ can be calculated as the cumulative sum of the PDF. Figure 11(b) illustrates the CDF for τ together with the threshold values corresponding to 16th and 50th percentiles of the probability distribution equal to 14.31, and 17.69, respectively.

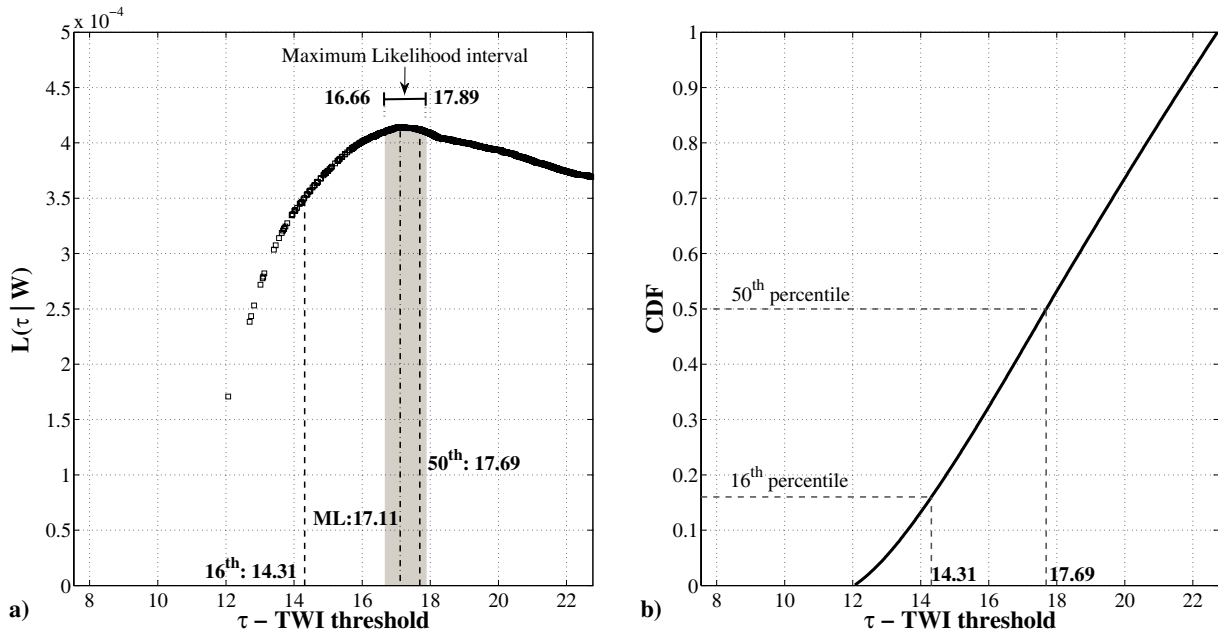


Figure 11 - a) The likelihood function $L(\tau|W)$ (also the probability density for τ); b) cumulative density function (CDF) for threshold value τ

A basic and visual check of the accuracy of the results (within window W) can be performed by overlaying the inundated zones (obtained from the hydraulic routine) and the TWI map for threshold values larger than the maximum likelihood estimate for τ denoted by τ_{ML} equal to 17.11 (i.e., $TWI > \tau_{ML}$). Figure 12 below illustrates for the local window W , the result of overlaying of hydraulic profile and $TWI > \tau_{ML}$ for T_R of 100.

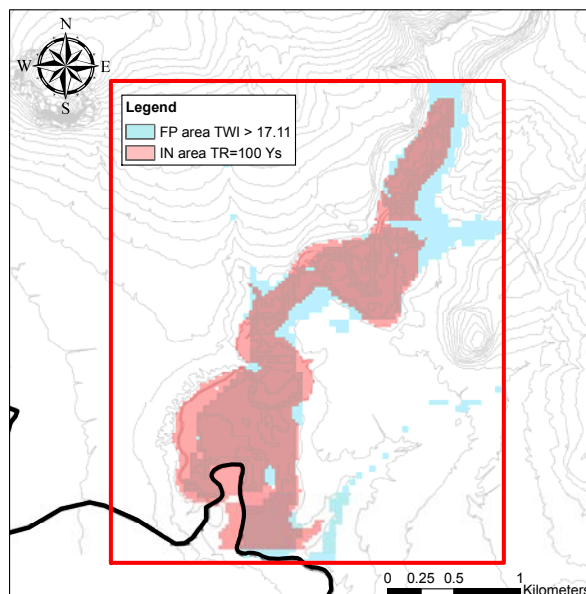


Figure 12 - Overlay of FP and IN areas for the spatial window W (Little Akaki).

The maximum likelihood estimation procedure is repeated also for the other return periods for which the hydraulic profiles have been calculated. The results are illustrated in Figure 12(a) and Figure 12(b) as the likelihood function and the cumulative distribution function for τ , respectively. As it can be depicted from Figure 12(a), the maximum likelihood estimate does not depend on the value of return period. Moreover, the cumulative distributions functions plotted for various return periods are almost identical. This is revealed also by examining the inundation profiles for various return periods in Figure 8. It can be observed that the delineation of the inundated areas is not sensitive to the return period (as opposed to the flood height that is sensitive to the return period). One possible interpretation is that the flood propagation extent depends on the topography of the area and not on the propagated flood volume.

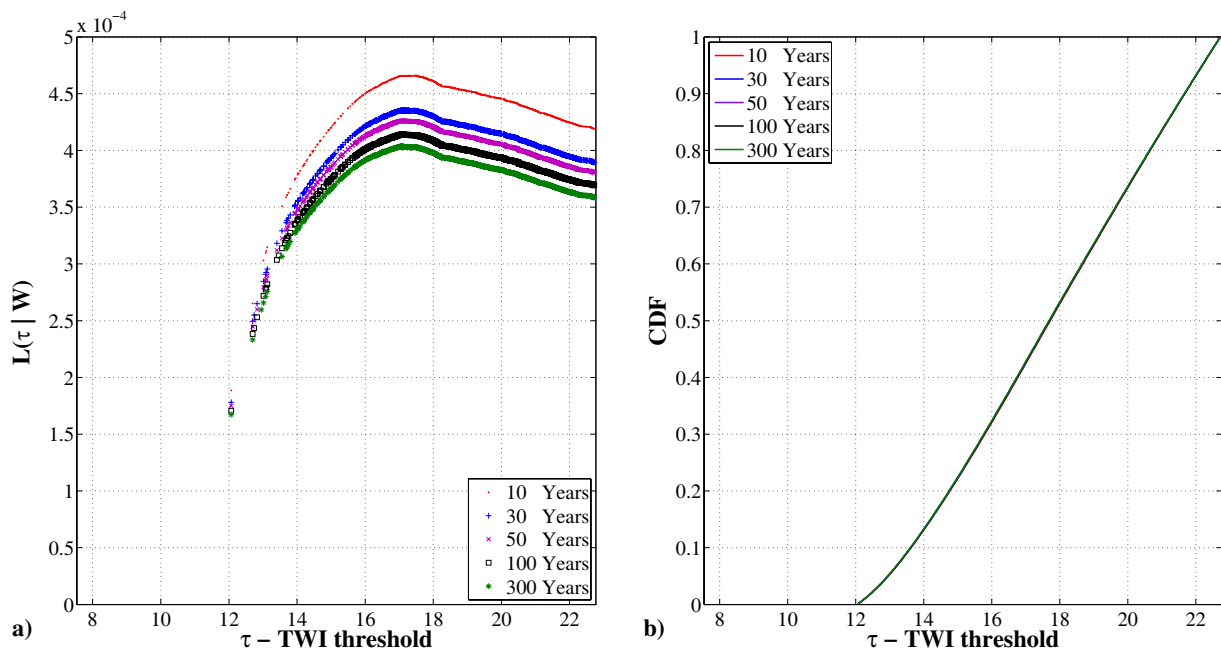


Figure 12 a) The likelihood function $L(\tau|W)$. b) threshold CDF for different return periods.

The above-mentioned discussion can be summarized in the following table that reports various statistics of the threshold value τ : the maximum likelihood estimate (ML), the 16th and 50th percentiles for TWI threshold and the 99% maximum likelihood interval $[\tau_{ML}^-, \tau_{ML}^+]$ for various return periods.

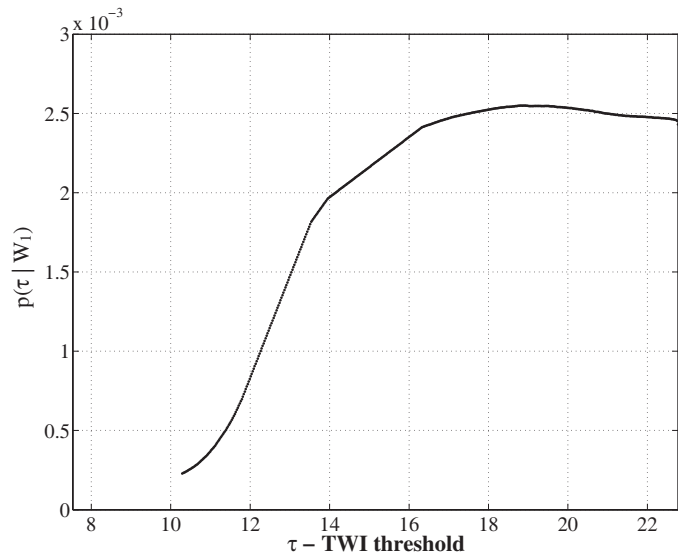
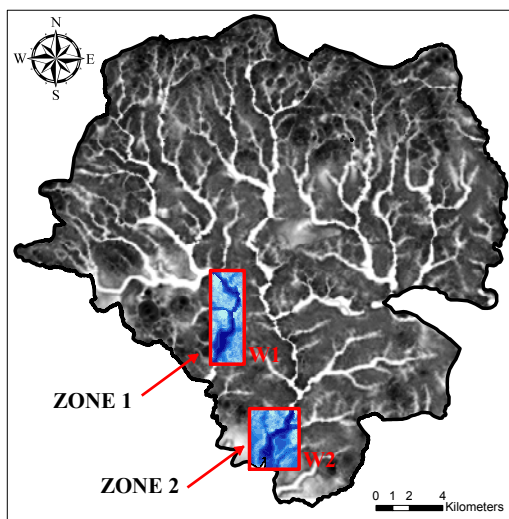
T_R	τ_{ML}	τ_{16}	τ_{50}	τ_{ML}^-	τ_{ML}^+
10	17.48	14.33	17.72	16.71	17.99
30	17.11	14.32	17.70	16.66	17.93
50	17.11	14.32	17.70	16.66	17.91
100	17.11	14.31	17.69	16.66	17.89
300	17.05	14.31	17.69	16.64	17.85

Table 1 - The statistics for the TWI threshold distribution as a function of the return period

Hereafter in this work, maximum likelihood threshold (τ_{ML}) equal to 17.05, 16th percentile (τ_{16}) equal to 14.31, 50th percentile (τ_{50}) equal to 17.69 and the 99% maximum values interval [16.64,17.85], are adopted.

3.1.4 Using Bayesian parameter estimation in order to estimate τ based on information from more than one spatial window

As mentioned, Eq. 9 can be used to calculate the threshold τ based on the inundation profiles for than one spatial window within the city. In the inundation profiles for $T_R=300$ yrs were available also for another zone of Addis herein referred to as Zone 1. This area is located between the subcities of Akaki (on the right) and Nefas Silk (on the left). Using the same procedure outlined in the previous section for the zone Little Akaki (hereafter referred to as Zone 2), the likelihood function for τ can be calculated. The probability density function τ denoted by $p(\tau|W_1)$ is plotted in Figure 13(b) below, recalling that the likelihood function $L((\tau|W_1)$ is equal to the probability density function for t (using a uniform prior $p(\tau)$ in Eq. 9). It can be observed that the distribution becomes almost uniform (in other words: *non informative*) for τ larger than about 17.



a)

b)

Figure 13 - a) Zones 1 and 2. b) $p(\tau|W_1)$:the posterior distribution calculated for Zone1 and used as prior for Zone 2

The posterior distribution $p(\tau|W_1)$ obtained for Zone 1, can be used as prior distribution for Zone 2, (the procedure outlined in the previous section is equivalent to using a uniform distribution). In Figure 14 below, the results based on inundation profiles calculated for Zone 2 (part (a), reported in the previous section) and the results based on inundation profiles calculated for Zone 1 and Zone 2 (part (b)) can be compared.

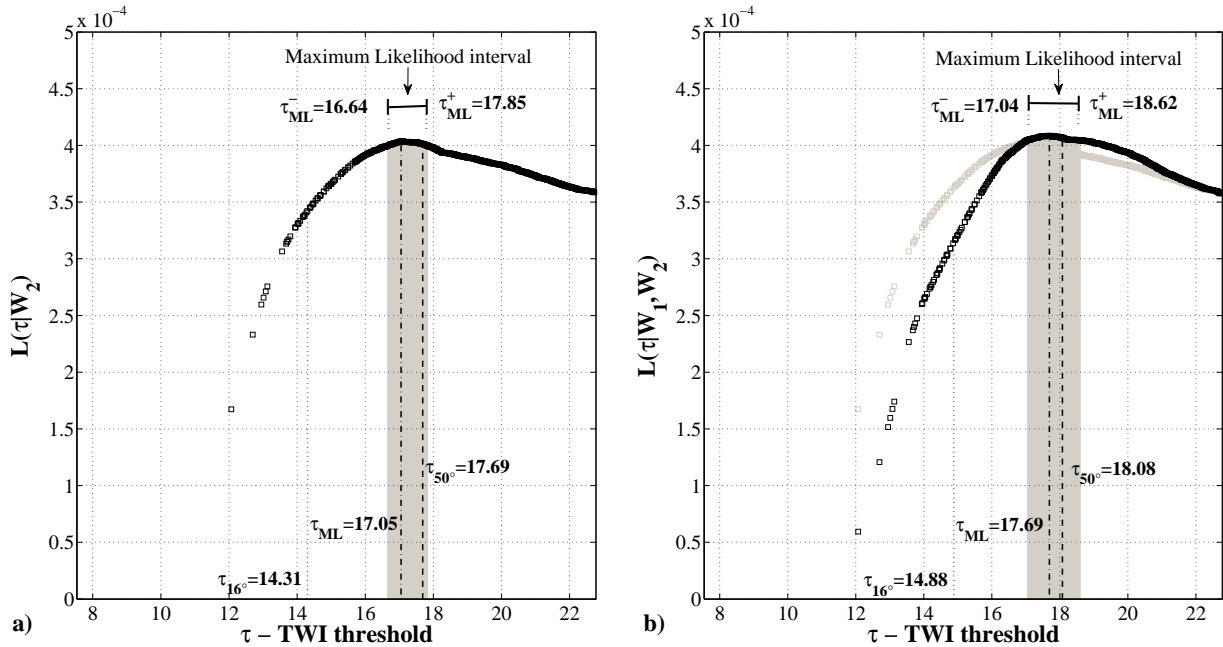


Figure 14 - a) the likelihood $L(\tau|W_2)$; b) the posterior distribution $p(\tau|W_1, W_2)$.

It can be observed that the statistics calculated for the TWI threshold do not change significantly by calibrating based on two spatial windows W_1 and W_2 ; for example, the τ_{ML} changes from 17.05 to 17.69. However, considering both spatial windows for calibration, leads to slightly wider 99% maximum likelihood interval for τ .

3.1.5 UMT for Addis Ababa city

The urban morphology types for Addis Ababa are classified and delineated based on aerial photos acquired in December 2010. Below in Figure 15, the high level UMT map for Addis Ababa is shown.

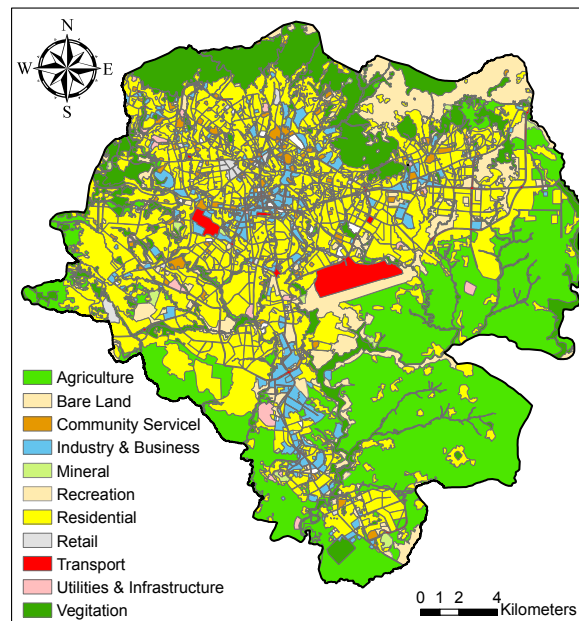


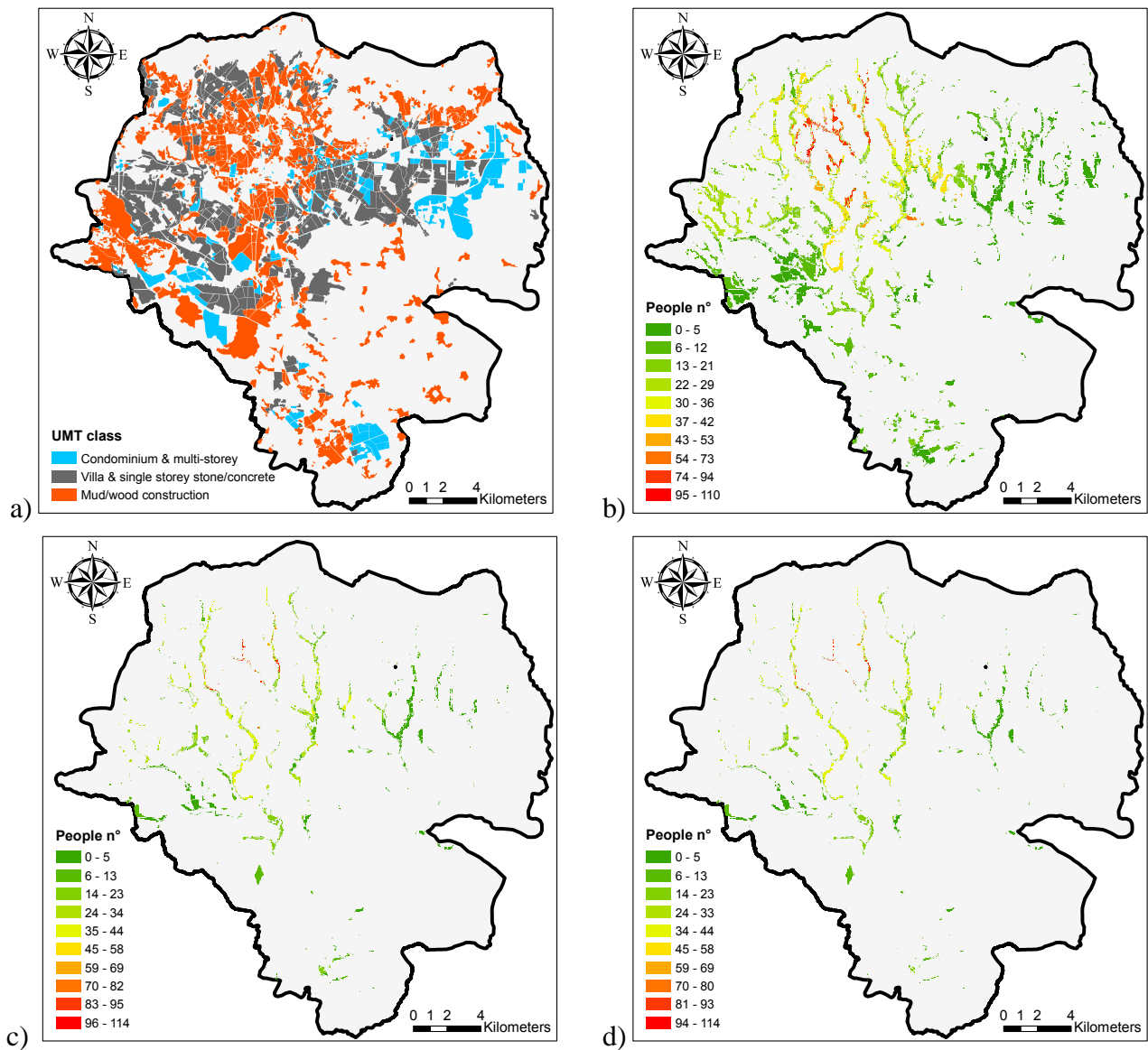
Figure 15 - High level UMT map for Addis Ababa (2011).

It can be observed that the field crops make up over one quarter of the area of the Addis Ababa study area, by far the largest area associated with a single sub-UMT category. Around over one third of the city is associated with UMT's classified as residential; among which, the mud/wood construction has the largest proportion (46%). About 3.4% of the city area is covered by major road corridors (i.e. width bigger than 15m). Although there is some evidence of an urban core, the UMT map provides further evidence of Addis Ababa's multi-nucleated character (Nvarirangwe 2008). There is a large proportion of bare land (9%); at least some of which is likely to be associated with future urban development. More detailed information about the identification of UMT sub-categories and the delineation of the UMT units for the city of Addis Ababa, reference is made to Cavan et al. (2012).

3.1.6 Identification of urban hotspots by overlaying the TWI and UMT datasets

The urban hot spots can be delineated by overlaying the flood prone areas and the urban morphology units classified as residential or major road corridors. Furthermore, integrating information from census results and/or field surveys/interviews, it will be also possible to estimate the exposure to flooding expressed as the estimated number of affected people.

The residential UMT: The spatial units characterized as residential cover about the 35% of the entire city surface; in which about the 46% of the population is concentrated. This category is further divided in three sub-categories: a) condominium and multi-storey buildings (cover the 5.3% of the city surface and contain the 4 % of the population), b) villa and single storey stone/concrete buildings (cover the 13.3% of the city surface and contain the 16% of the population), and c) mud and wood construction (cover the 16.1% of the city surface and contain the 26% of the population). Figure16 illustrates the delineated urban hotspots (the coloured zones), obtained by overlaying the UMT and the TWI datasets, for different estimates of TWI threshold.



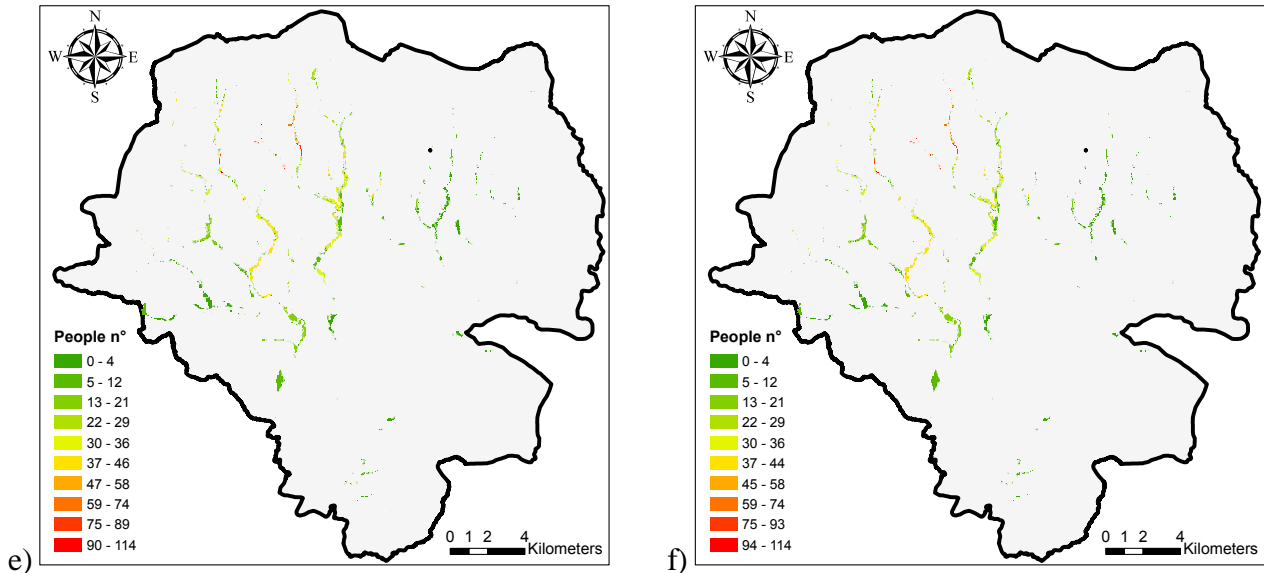


Figure 16 - The urban residential hot spots for flooding delineated for different TWI thresholds: a) residential area, b) 16th percentile, c) τ_{ML}^- , d) maximum likelihood, e) 50th percentile, f) τ_{ML}^+ .

Furthermore, the information on population density obtained from the city census (2007) is integrated in order to estimate the number of affected people by flooding for different statistics of the TWI threshold. Table 2 below demonstrates the percentage of residential area affected by flooding (the areal extent of hot spots illustrated in Figure 16 normalized by total residential area) and the percentage of people that live in the residential area affected (estimated population normalized by total population in the residential area), for different estimates of the TWI threshold.

% of Residential	τ_{ML}	τ_{16}	τ_{50}	τ_{ML}^-	τ_{ML}^+
Area	4.64%	22.18%	3.07%	5.96%	2.74%
People	5.59%	26.86%	3.67%	7.11%	3.31%

Table 2 - Exposure to flooding risk in terms of the estimated percent of residential area and people affected by flooding

It can be noted that the percentages of people affected to flooding for Addis Ababa in correspondence to τ_{50} and τ_{16} varies in the interval [2.60%, 12.50%] of the total Addis Ababa population. This⁵ can be interpreted as the 50th and 84th percentiles of the number of people (in the residential areas) affected to flooding. In particular, the 84th percentile (12.50% of 2.8 millions) of the number of people affected in the residential areas is about 350,000 people which can be compared (as a means of back analysis) to the total number of people affected in the 2007 flooding.

% of City	τ_{ML}	τ_{16}	τ_{50}	τ_{ML}^-	τ_{ML}^+
People	2.60%	12.49%	1.71%	3.31%	1.54%

⁵ If the process of calculating the number of affected people is strictly monotonic, the percentiles of threshold value would be translated directly into the same percentiles for the estimated number of people.

Discussion:

The pie chart shown in Figure 17 below illustrates the percentage break-down of the residential hot spots areal extent (corresponding to τ_{ML} equal to 17.05) in terms of different residential sub-classes; namely, a) condominium/multi-storey, b) single storey stone/concrete and c) mud/wood construction.

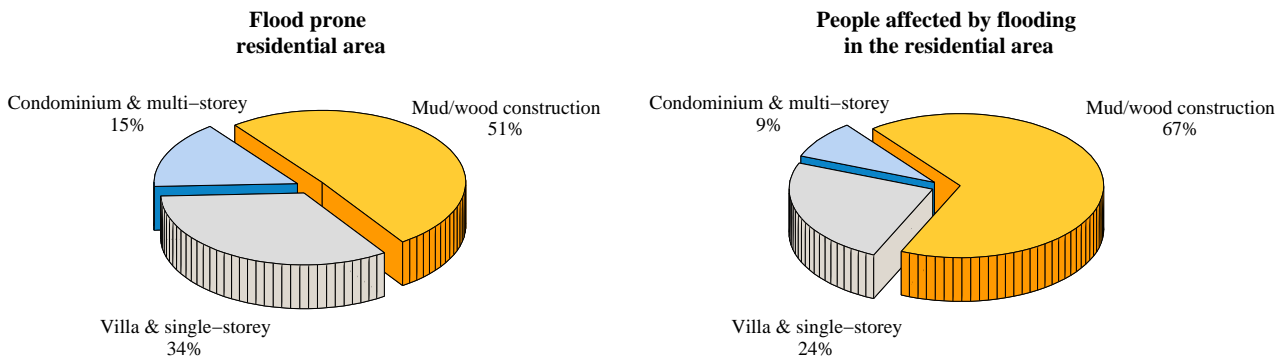


Figure 17 - Breakdown of the residential hot-spot in terms of flood prone residential area and people affected by flooding in the residential area.

It can be observed that 67% of the population in the flood prone residential area lives in mud and wood constructions (constituting 51% of total residential area) that are particularly vulnerable to flood action.

The major road corridors UMT: The UMT class "major road corridors" covers about 3.4% of the whole city surface. Below in Figure 18, the delineated urban road corridor hotspots (the red zones) are shown for different estimates of TWI threshold.

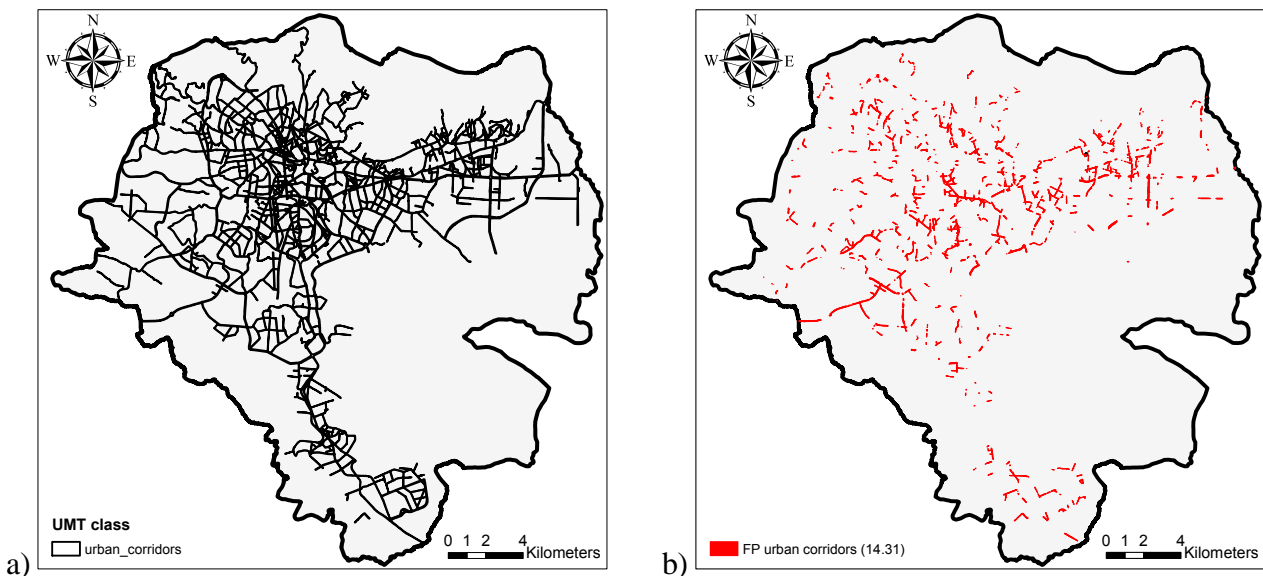




Figure 18 - The urban corridor hot spots for flooding delineated for different TWI thresholds: a) residential area, b) 16th percentile, c) τ_{ML}^- , d) maximum likelihood, e) 50th percentile, f) τ_{ML}^+ .

Table 3 below reports the percentage of roads affected by flooding (estimated as the extent of red hot spots illustrated in Figure 18 normalized by total urban corridors area) for different estimates of the TWI threshold.

% of Urban Corridors Area	τ_{ML}	τ_{16}	τ_{50}	τ_{ML}^-	τ_{ML}^+
	5.18%	23.45%	3.38%	6.93%	2.92%

Table 3 - Exposure assessment in terms of urban corridors

3.2 THE CASE OF DAR ES SALAAM

The city of Dar Es Salaam in Tanzania is located between latitudes 6.36° and 7.0° to the South of Equator and longitudes 39.0° and 33.33° to the East of Greenwich. It borders Indian Ocean on the east and its coastline stretches about 100 km between the Mpiji River to the north and the Mzinga River in the south. The total surface area of Dar Es Salaam city is about 1800 km^2 , comprising of 1393 km^2 of land mass with eight offshore islands, which is about 0.19% of the entire Tanzania Mainland's area. Administratively, Dar Es Salaam City is divided into three municipalities and Districts of Kinondoni, Ilala and Temeke, with a total population of 2698651 according to the 2005 population census.

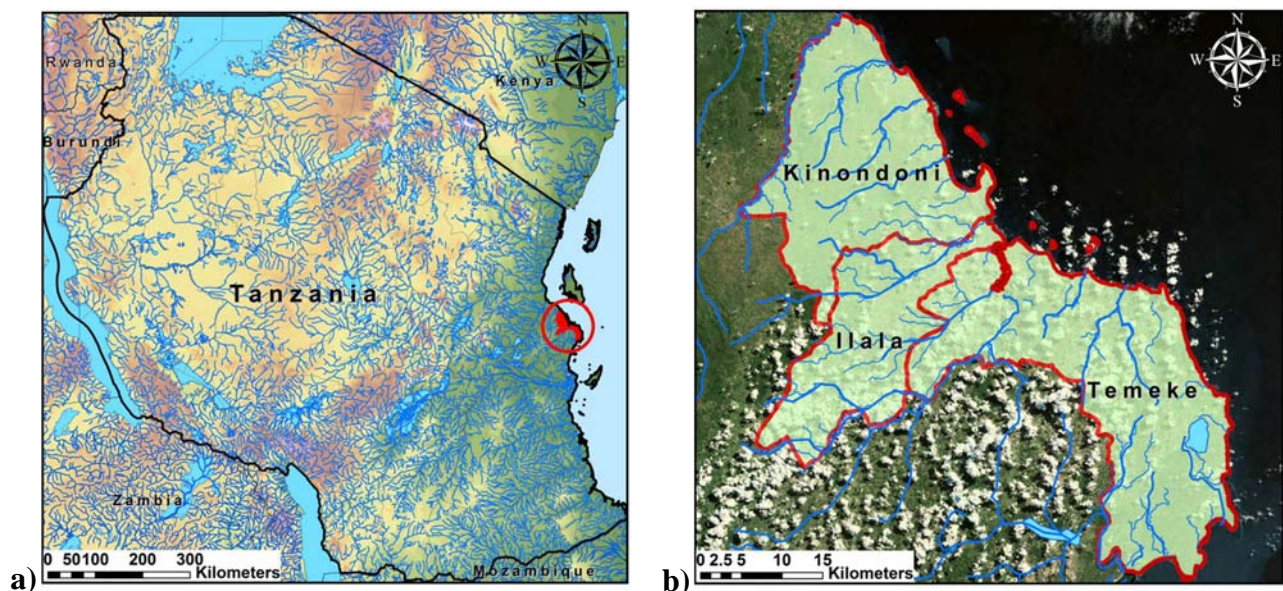


Figure 19 - a) Tanzania, b) Dar Es Salaam city

3.2.1 Delineation of flood-prone areas for Dar Es Salaam using the topographic wetness index (TWI)

The topographic wetness index is calculated in the GIS framework by applying Eq. 1 and based on the digital elevation model of the city (Year: 2008, vertical resolution: 10 meters, reduced to 10 meters through the spatial interpolation). Figure 20 illustrates the resulting TWI map for Dar. It can be observed that the TWI values vary between 10.34 and 22.78; in particular, largest TWI values can be spotted around the natural water channels.

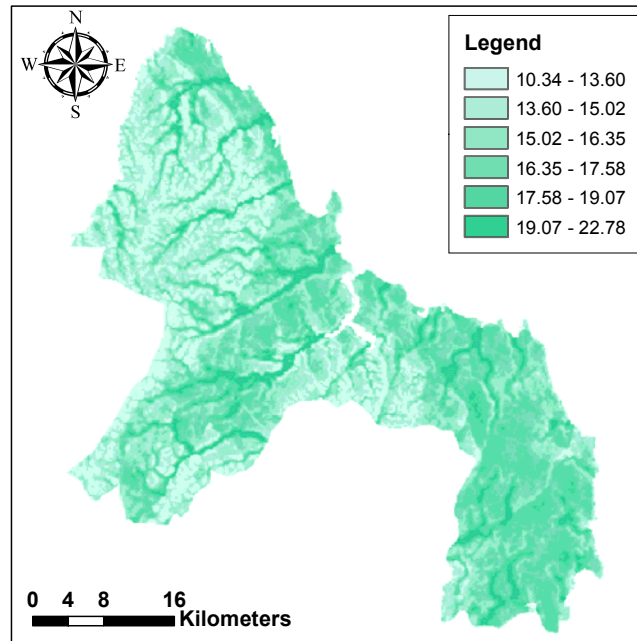


Figure 20 - TWI for Dar Es Salaam

3.2.2 *The inundation profile for Suna*

In order to calibrate the TWI threshold for Dar Es Salaam, the inundation profile for various return periods have been calculated for Suna located in between Ilala and Kinondoni districts. Suna results as flood-prone based on past flooding experiences. The inundation profile has been calculated by bi-dimensional simulation of flood volume propagation using the software FLO2D (using historical rainfall records, the DEM, and the calculation of the hydrograph based on the curve number method) assuming a simulation time of 45 hours. The outcome of the flood propagation is illustrated in Figure 21 in terms of maximum flow depth h_{max} with reference to six considered return periods (T_R 2, 10, 30, 50, 100 and 300 years).

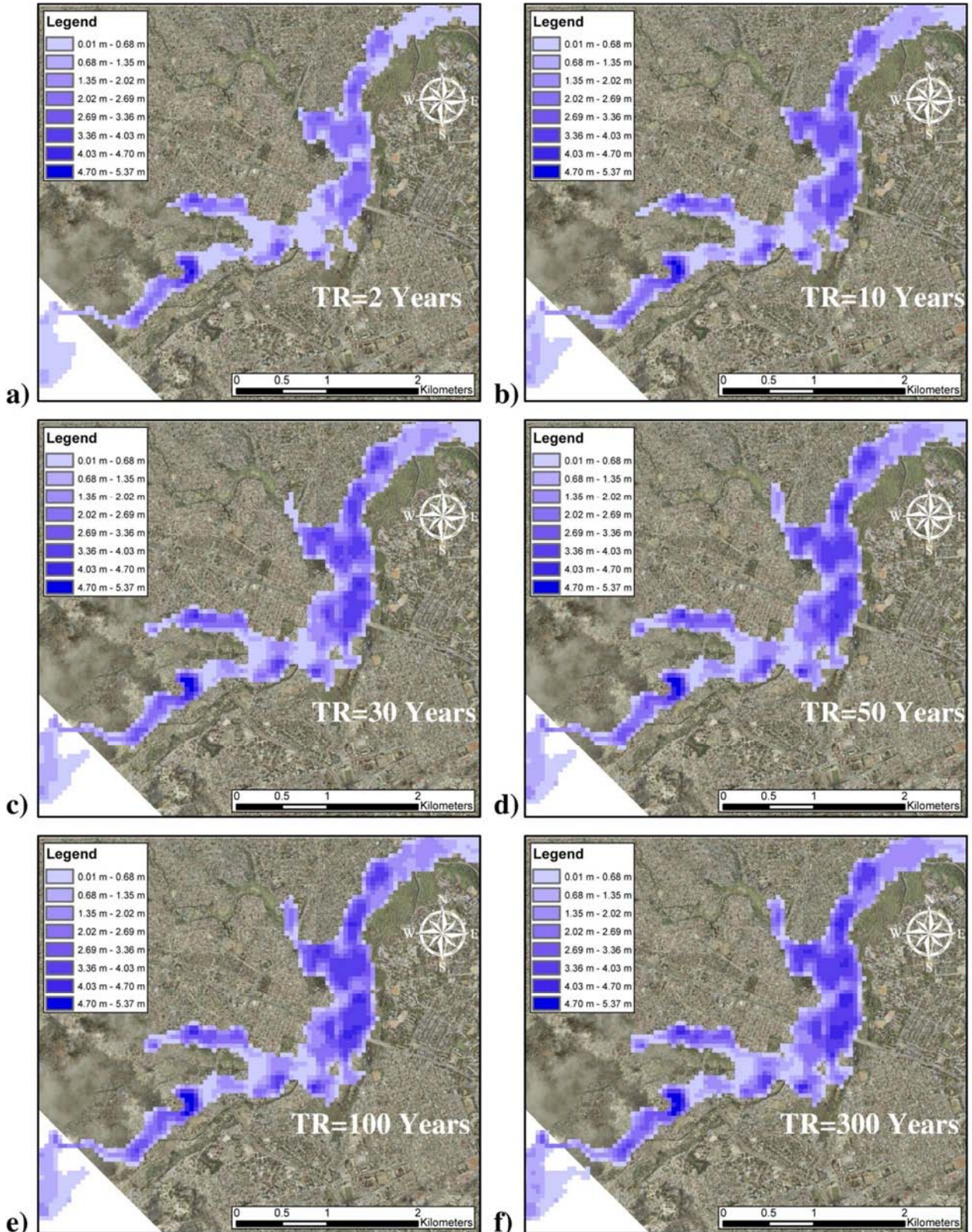


Figure 21 - Inundation profiles in terms of h_{max} [in meters] for various return periods for the case study area

3.2.3 Maximum likelihood estimation of the flood-prone threshold

In this section, it is demonstrated how the procedure described previously in the methodology can be applied in order to calculate the likelihood of being flood prone as a function of the TWI threshold.

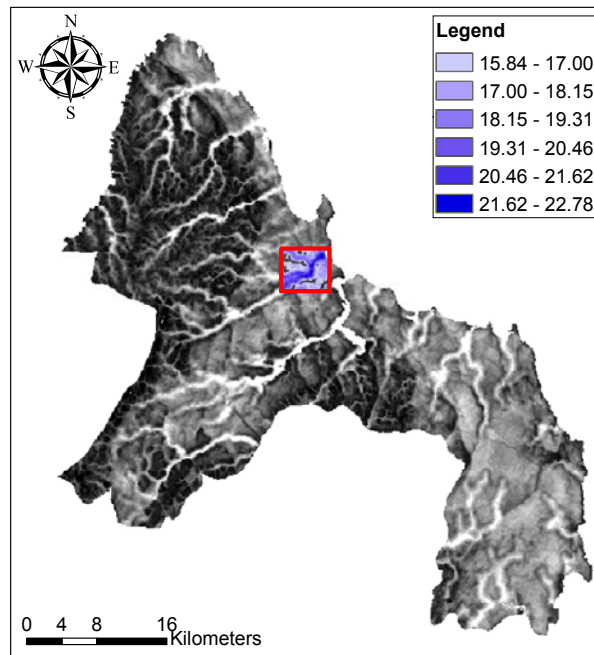


Figure 22 - The TWI and the spatial the window for hydraulic analyses at Suna

A spatial window identified as W with $A(W)$ around 27 km^2 is defined in the zone of Suna (Figure 22). For a return period $T_R=100$ years and for all the possible values of τ , the probability that a given zone is flood prone $P(\text{FP}|\tau)$ is calculated from Eq. 8 (based on meso-scale estimations) and is plotted in Figure 23(a) (as the black dots). Moreover, the probability that a given point is inundated $P(\text{IN}|\text{FP}, \tau)$ given that it is already indicated as FP for a given value of τ is calculated from Eq. 6 (based on micro-scale estimations) and plotted in Figure 23(a) (as the stars in gray). The probability that a given point is indicated both as flood prone (by the TWI method) and inundated (based on the hydraulic profile), $P(\text{FP}, \text{IN}|\tau)$ is calculated from Eq. 4 as the product of $P(\text{FP}|\tau)$ and $P(\text{IN}|\text{FP}, \tau)$ from Eq. 4 and plotted in Figure 23(a) (as the circles in red). In a similar manner, the probability that a given point is not indicated as flood prone based on the TWI method is calculated as the complementary probability of being flood prone in Eq. 8 and plotted in Figure 23(b) (as the black dots). The probability that a given zone is not indicated as inundated given that it is not flood prone for a given value of τ is calculated from Eq. 7 and is plotted as the gray stars in Figure 23(b). Finally the probability that a given point is not inundated and not flood prone for a given value of τ , is calculated from Eq. 5 and plotted as the red circles in Figure 23(b).

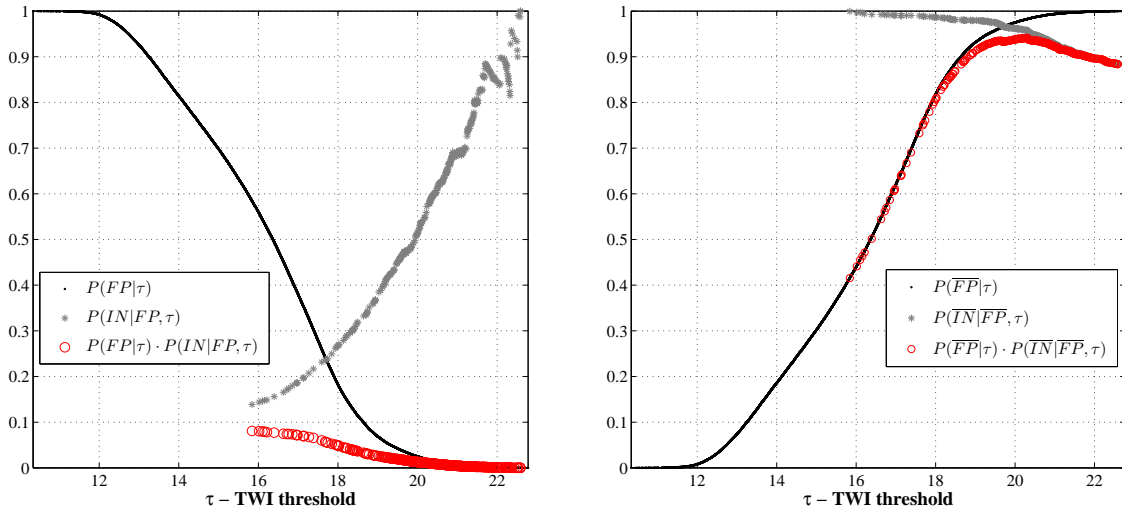


Figure 23 - a) Probability of being FP and IN given τ . b) Probability of being \overline{FP} and \overline{IN} given τ .

The likelihood function for window W at $T_R=100$ years is finally calculated from Eq. 2 by summing up the probability of being flood prone and inundated and the probability of not being flood prone and not being inundated for all possible τ values (i.e., summing up the curves illustrated by red circles in Figure 23(a) and Figure 23(b)). It is noteworthy that the probability $P(FP|\tau)$ and its complement are both defined in the domain of the threshold values ranging between 10.34 and 22.78 (the meso-scale estimations, Figure 21). Instead, the terms $P(IN|FP, \tau)$ and $P(\overline{IN}|\overline{FP}, \tau)$ are defined in the domain ranging between 15.84 and 22.78 (the micro-scale estimations, Figure 22).

The resulting likelihood function $L(\tau|W)$ is plotted in Fig. 24(a) as a function of the TWI threshold τ . Consequently, the maximum likelihood estimate for τ (i.e., the value that corresponds to the maximum likelihood) can be identified as $\tau=19.53$. Furthermore, by identifying the τ values corresponding to 99% of the maximum likelihood value, it is possible to define a maximum likelihood interval, that varies between $\tau_{ML}^- = 19.16$ and $\tau_{ML}^+ = 20.44$. That is, from a practical point of view, the information used for calibrating the TWI threshold lead to identifying a maximum likelihood interval [19.16, 20.44] for τ .

Recalling that the likelihood function also represents the probability density function (PDF) for τ , the cumulative distribution for τ can be calculated as the cumulative sum of the PDF. Figure 24(b) illustrates the CDF for τ together with the threshold values corresponding to 16th and 50th percentiles of the probability distribution equal to 17.31, and 19.50, respectively.

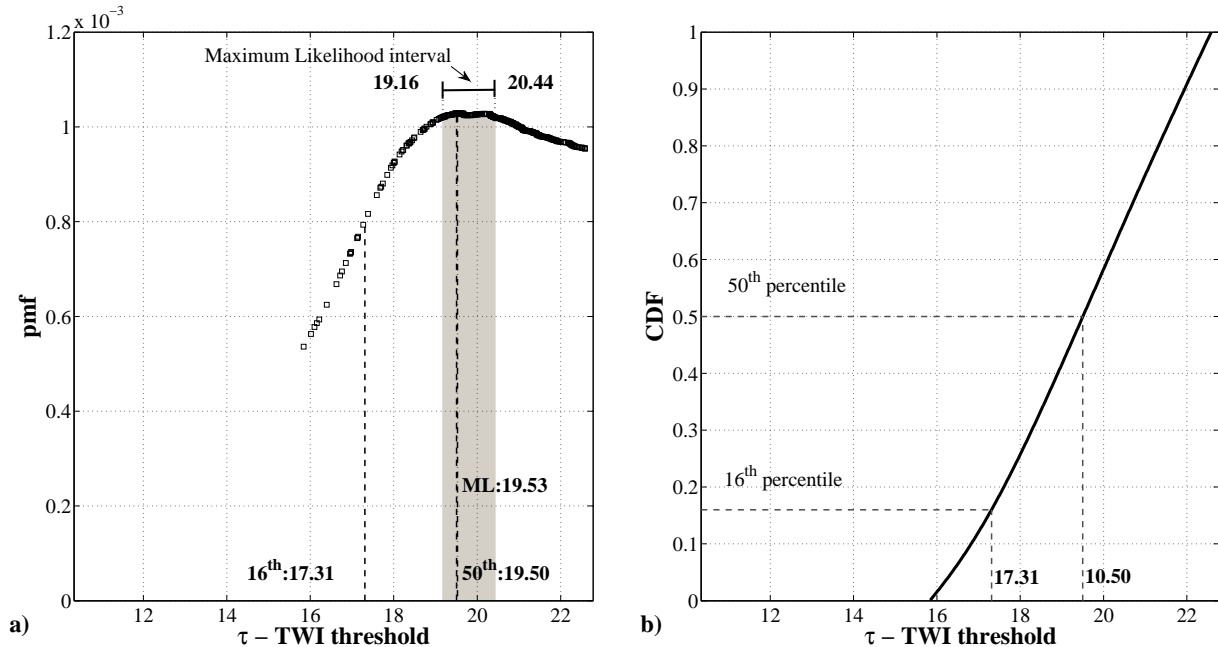


Figure 24 - a) The likelihood function $L(\tau|W)$ (also the probability density for τ); b) threshold CDF.

A basic and visual check of the accuracy of the results (within window W) can be performed by overlying the inundated zones (obtained from the hydraulic routine) and the TWI map for threshold values larger than the maximum likelihood estimate for τ denoted by τ_{ML} equal to 19.53 (i.e., $\text{TWI} > \tau_{ML}$). Figure 25 below illustrates for the local window W , the result of overlaying of hydraulic profile and $\text{TWI} > \tau_{ML}$ for T_R of 100.

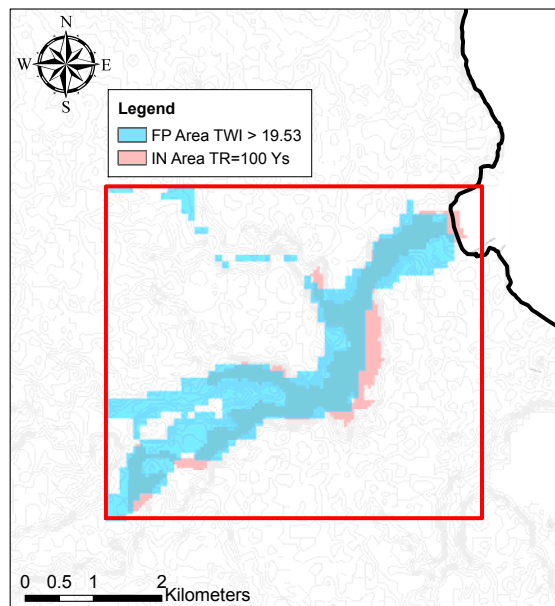


Figure 25 - Overlay of FP and IN areas for the spatial window W .

The maximum likelihood estimation procedure is repeated also for the other return periods for which the hydraulic profiles have been calculated. The results are illustrated in Figure 26(a) and Figure 26(b) as the likelihood function and the cumulative distribution function for τ , respectively. As it can be depicted from Figure 26(a), the maximum likelihood estimate does not depend on the value of return period. Moreover, the cumulative distributions functions plotted for various return periods are almost identical. This is revealed also by examining the inundation profiles for various return periods in Figure 21. It can be observed that the delineation of the inundated areas is not sensitive to the return period (as opposed to the flood height that is sensitive to the return period).

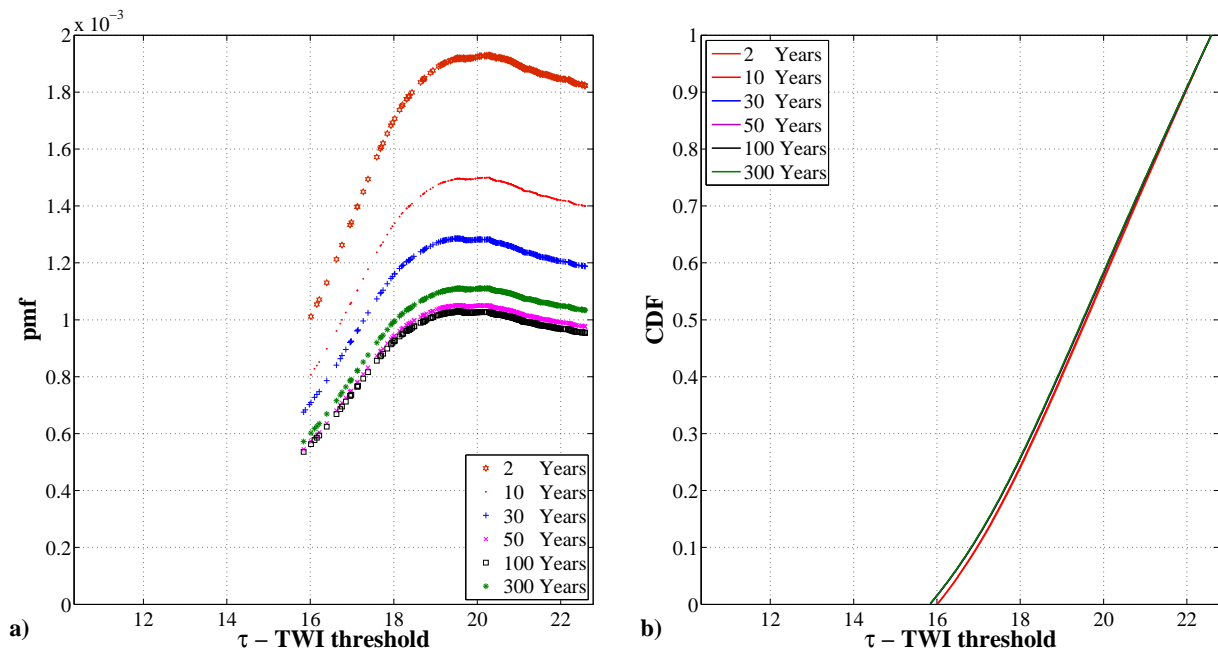


Figure 26 - a) The likelihood function $L(\tau|W)$. b) threshold CDF for different return periods.

The above-mentioned discussion can be summarized in the following table that reports various statistics of the threshold value τ : the maximum likelihood estimate (ML), the 16th and 50th percentiles for TWI threshold and the 99% maximum likelihood interval $[\tau_{ML}^-, \tau_{ML}^+]$ for various return periods.

T_R	τ_{ML}	τ_{16}	τ_{50}	τ_{ML}^-	τ_{ML}^+
2	20.28	17.44	19.59	19.40	20.81
10	20.28	17.42	19.57	19.24	20.60
30	20.17	17.32	19.51	19.17	20.57
50	19.53	17.31	19.51	19.16	20.46
100	19.53	17.31	19.50	19.16	20.44
300	19.53	17.30	19.50	19.12	20.40

Table 4 - The statistics for the TWI threshold distribution as a function of the return period

Hereafter in this work, maximum likelihood threshold (τ_{ML}) equal to 19.53, 16th percentile (τ_{16}) equal to 17.30, 50th percentile (τ_{50}) equal to 19.50 and the 99% maximum values interval [19.12,20.40], are adopted.

3.2.4 UMT for Dar es Salaam

The urban morphology types for Dar es Salaam are classified and delineated based on aerial photos acquired in December 2010. Below in Figure 27, the high level UMT map for Dar is shown.

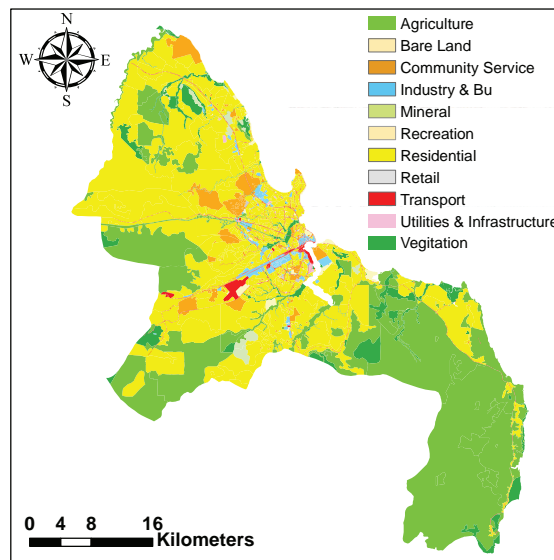


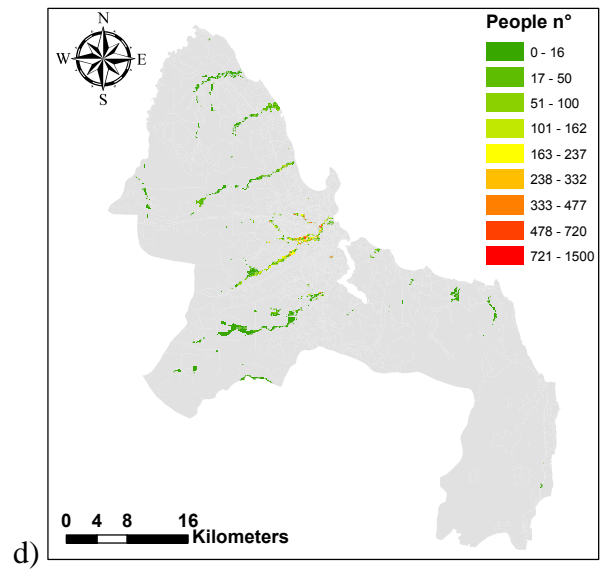
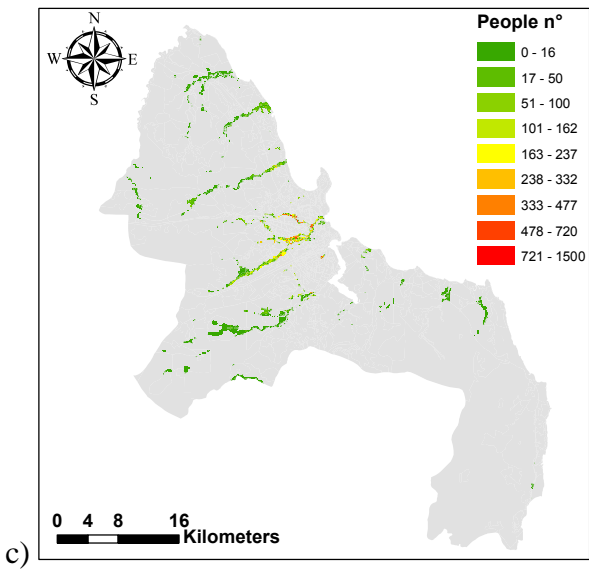
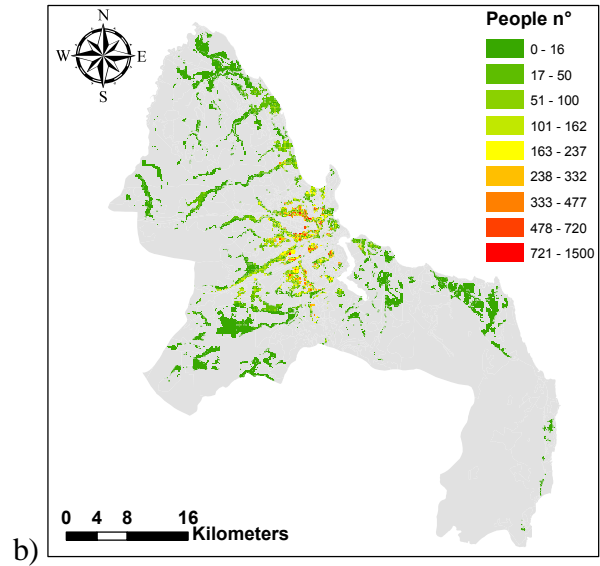
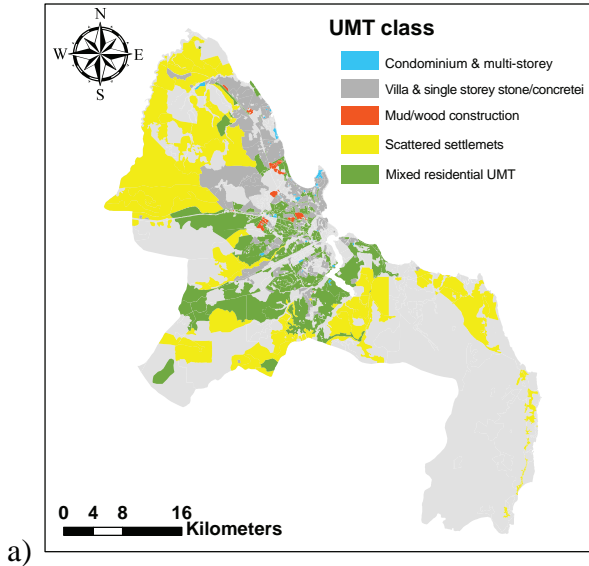
Figure 27 - High level UMT map for Dar es Salaam.

3.2.5 Identification of urban hotspots by overlaying the TWI and UMT datasets

The urban hot spots can be delineated by overlaying the flood prone areas and the urban morphology units classified as residential or major road corridors. Furthermore, integrating information from census results and/or field surveys/interviews, it will be also possible to estimate the exposure to flooding expressed as the estimated number of affected people.

The residential UMT: The spatial units characterized as residential cover about the 47% of the entire city surface; in which about the 60% of the population is concentrated. This category is further divided in five sub-categories: a) condominium and multi-storey buildings (cover the 0.2% of the city surface and contain the 0.5 % of the population), b) villa and single storey stone/concrete buildings (cover the 7.8% of the city surface and contain the 17% of the population), c) mud and wood construction (cover the 0.4% of the city surface and contain the 2% of the population), d) scattered settlement (cover the 25% of the city surface and contain the 5.3% of the population) and e) mixed residential (cover the 13% of the city and contain the 36% of the population).

Fig. 28 illustrates the delineated urban hotspots (the colored zones), obtained by overlaying the UMT and the TWI datasets, for different estimates of TWI threshold.



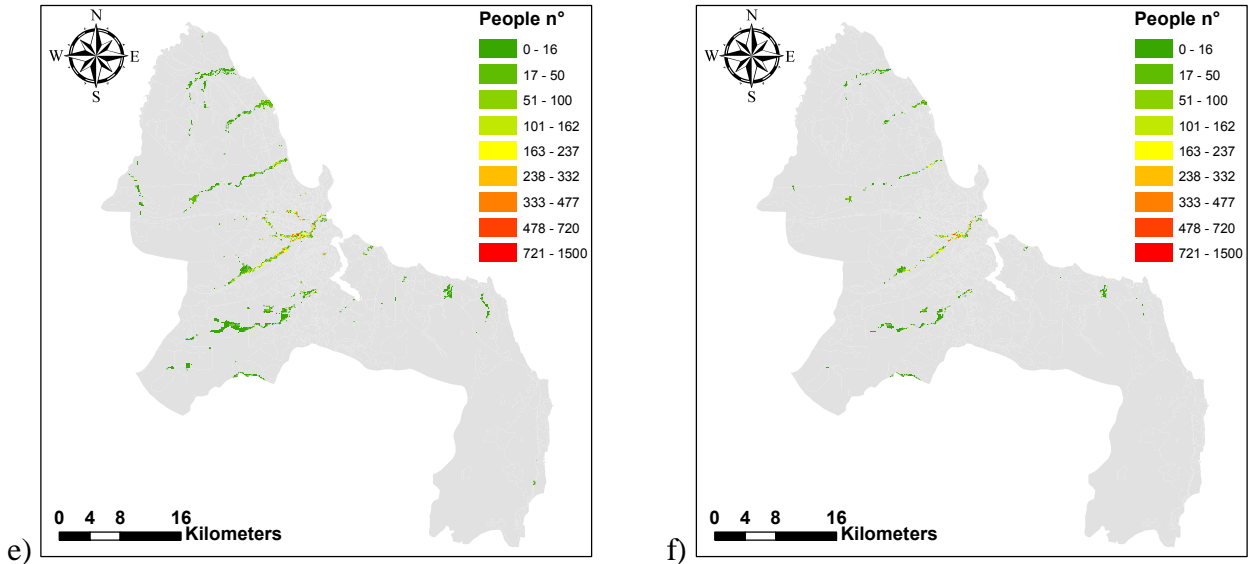


Figure 28 - The urban residential hot spots for flooding delineated for different TWI thresholds: a) residential area, b) 16th percentile, c) τ_{ML}^- , d) maximum likelihood, e) 50th percentile, f) τ_{ML}^+ .

Furthermore, the information on population density obtained from the city census (2005) is integrated in order to estimate the number of affected people by flooding for different statistics of the TWI threshold. Table 5 below demonstrates the percentage of residential area affected by flooding (the areal extent of hot spots illustrated in Figure 28 normalized by total residential area) and the percentage of people that live in the residential area affected (estimated population normalized by total population in the residential area), for different estimates of the TWI threshold.

% of Residential	τ_{ML}	τ_{16}	τ_{50}	τ_{ML}^-	τ_{ML}^+
Area	3.45%	23.08%	3.53%	4.93%	1.31%
People	6.35%	37.76%	6.48%	9.14%	2.44%

Table 5 - Exposure to flooding risk in terms of the estimated percent of residential area and people affected by flooding

It can be noted that the percentages of people affected to flooding for Dar es Salaam in correspondence to τ_{50} and τ_{16} varies in the interval [1.48%, 22.91%] of the total Dar es Salaam population. This⁶ can be interpreted as the 50th and 84th percentiles of the number of people (in the residential areas) affected to flooding. In particular, the 84th percentile (12.50% of 2.8 millions) of the number of people affected in the residential areas is about 620000 people.

% of City	τ_{ML}	τ_{16}	τ_{50}	τ_{ML}^-	τ_{ML}^+
People	3.85%	22.91%	3.93%	5.54%	1.48%

⁶ If the process of calculating the number of affected people is strictly monotonic, the percentiles of threshold value would be translated directly into the same percentiles for the estimated number of people.

Discussion:

The pie chart shown in Figure 29 below illustrates the percentage break-down of the residential hot spots areal extent (corresponding to τ_{ML} equal to 19.53) in terms of different residential sub-classes; namely, a) condominium/multi-storey, b) single storey stone/concrete and c) mud/wood construction, d) scattered settlement and e) mixed residential.

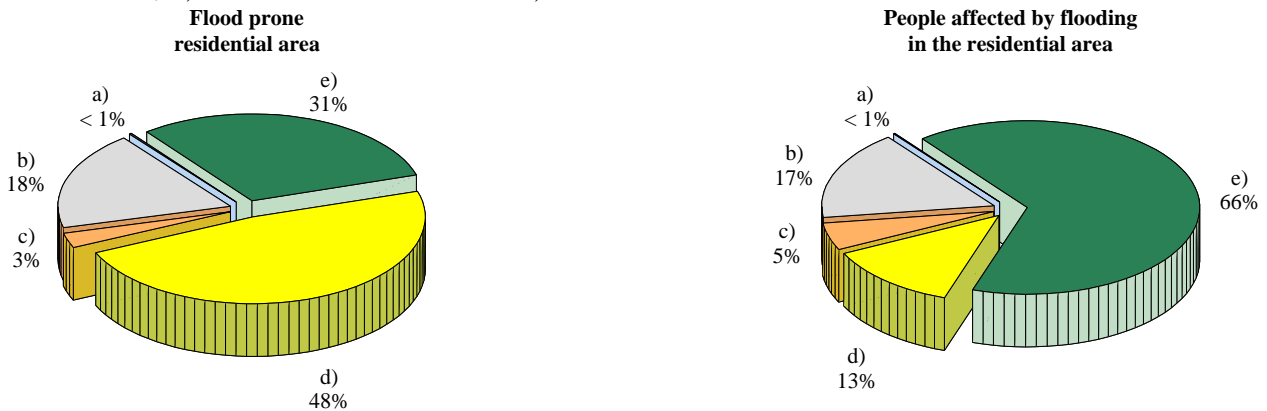
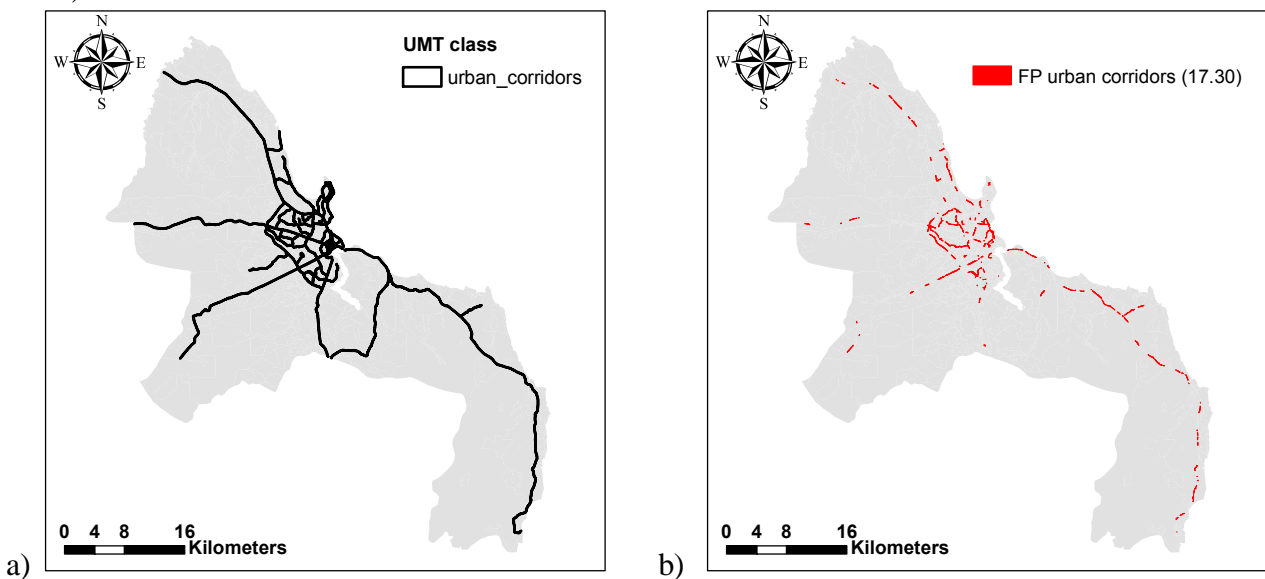


Figure 29 - Breakdown of the residential hot-spot in terms of flood prone residential area and people affected by flooding in the residential area.

It can be observed that around 66% of the population in the flood prone residential area lives in residential types labeled as *mixed*. This residential type constitutes around 31% of the flood-prone residential buildings. On the other hand, around half of the buildings identified as flood-prone belong to the scattered settlements category. Moreover, the inhabitants of the scattered settlements constitute around 13% of the total population affected by flooding.

The major road corridors UMT: The UMT class "*major road corridors*" covers about 0.5% of the whole city surface. Below in Figure 30, the delineated urban road corridor hotspots (the red zones) are shown for different estimates of TWI threshold.



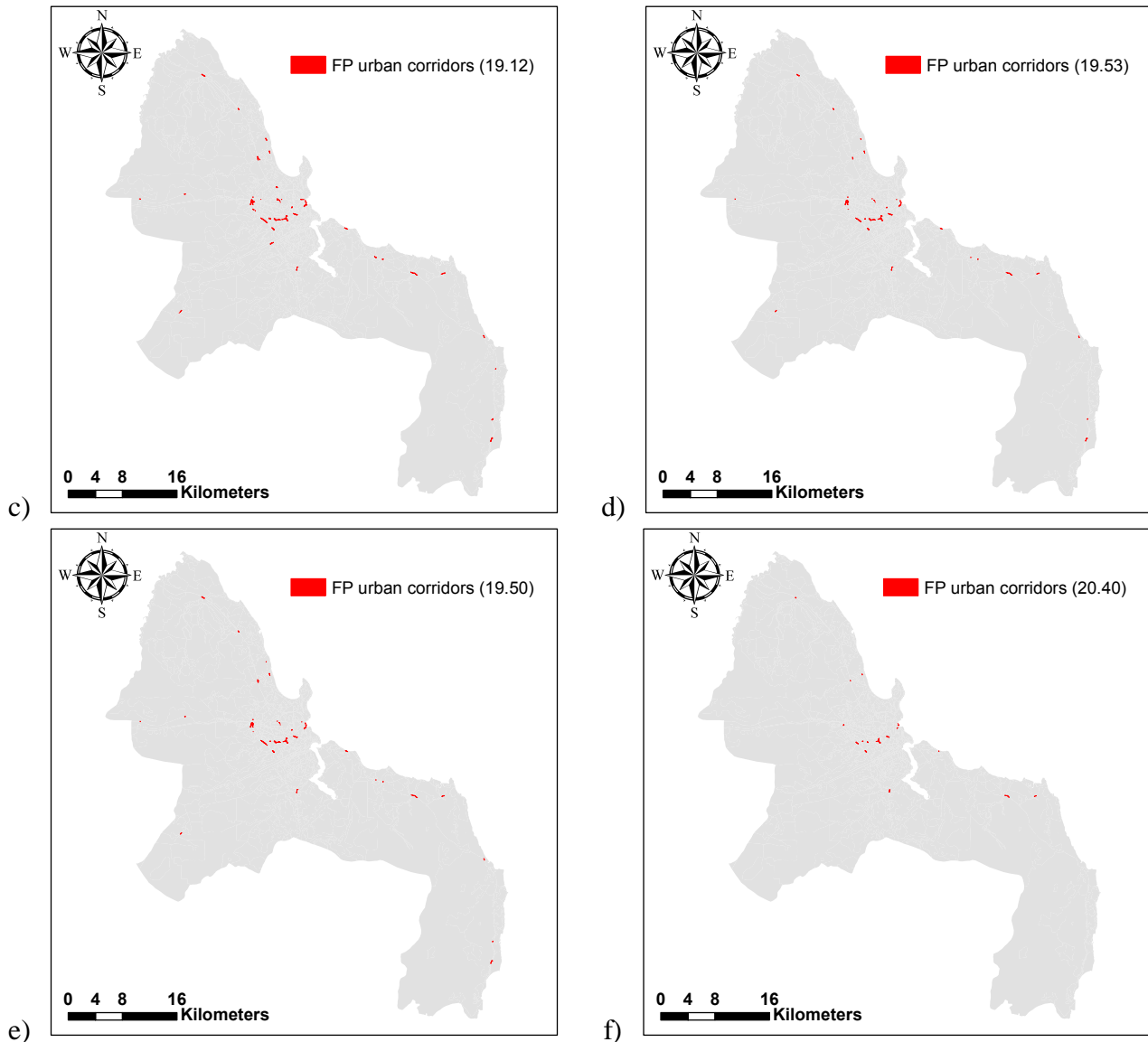


Figure 30 - The urban corridor hot spots for flooding delineated for different TWI thresholds: a) residential area, b)16th percentile, c) τ_{ML}^- , d)maximum likelihood, e) 50th percentile, f) τ_{ML}^+ .

Table 6 below reports the percentage of roads affected by flooding (estimated as the extent of red hot spots illustrated in Figure 30 normalized by total urban corridors area) for different estimates of the TWI threshold.

% of Urban Corridors Area	τ_{ML}	τ_{16}	τ_{50}	τ_{ML}^-	τ_{ML}^+
	3.80%	29.81%	3.93%	5.87%	1.54%

Table 6 - Exposure assessment in terms of urban corridors

It can be observed that around 66% of the population in the flood prone residential area lives in residential types labeled as *mixed*. This residential type constitutes around 31% of the flood-prone residential buildings. On the other hand, around 50% of the flood-prone buildings belong to the scattered settlements category which have house around 13% of the flood-prone population.

3.2.6 Procedure validation

In order to visually investigate and validate the hot spot identification results for flood-prone residential buildings, we have overlaid the map of a group of flood-prone informal settlements (established based on house-hold interviews) in Suna (Dar es Salaam) and a zoom-in of the hot-spot map reported in Figure 28(d). Figure 31 illustrates the results. The color gradation reflects the population density.

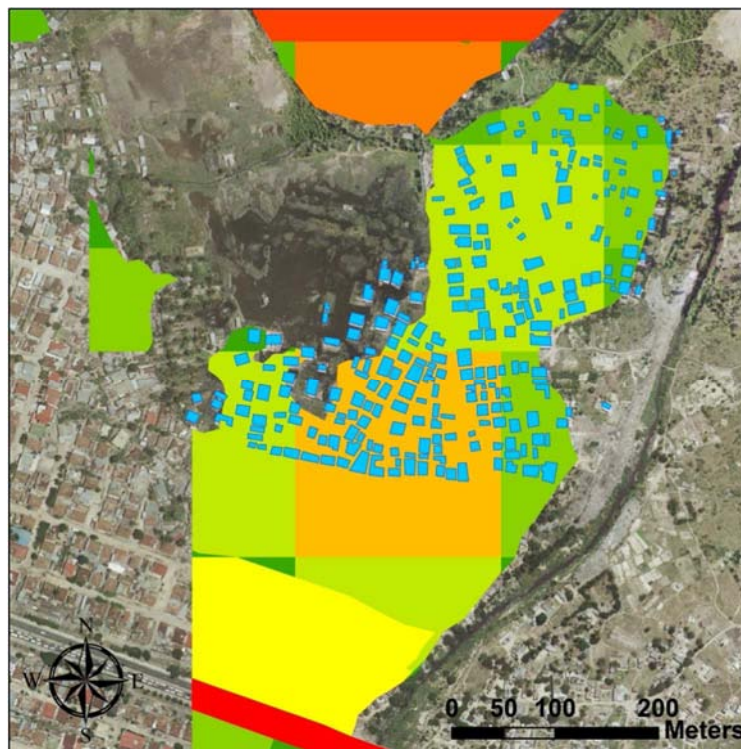


Figure 31 - Overlay of the urban residential flood hotspots map zoomed in to Suna (DSM) and a group of houses identified as flood-prone based on house-hold interviews (highlighted on an orthophoto).

3.3 THE CASE OF OUGADOUGOU

Ouagadougou is the capital of the Burkina Faso. It has a population of around 1 million and a half and covers an area of 219.3 km².



Figure 32 - Burkina Faso, with Ouagadougou position (in red)

On September 1, 2009, an unprecedented deluge of rain hit the capital city of Ouagadougou and resulted in wide-spread damage (destruction of buildings and infrastructure). More than 25 cm of rainfall in 12 hours turned the streets of Ouagadougou into fast-flowing rivers. The infrastructure were severely affected as the floods cut off electricity, fresh water and fuel supplies. The city is used to heavy seasonal rainfall but this was the worst flooding in 50 years. An estimated 109.000 people were left homeless. (CLUVA Deliverable **D5.2**)

3.3.1 Delineation of flood-prone areas for Ouagadougou using the topographic wetness index (TWI)

The topographic wetness index is calculated in the GIS framework by applying Eq. 1 and based on the digital elevation model of the city (Vertical resolution: 3 meters). Figure 33 illustrates the resulting TWI map for Ouagadougou. It can be observed that the TWI values vary between 8 and 25; in particular, largest TWI values can be spotted around the natural water channels.

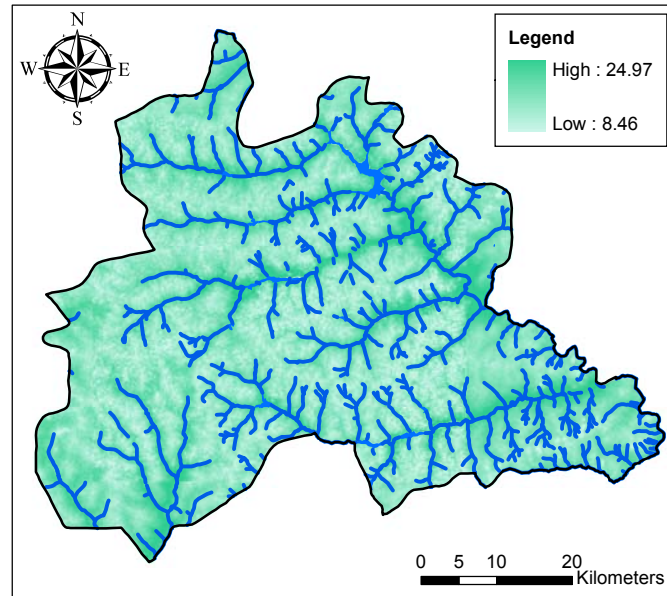


Figure 33 - TWI for Ouagadougou

3.3.2 The inundation profile

In contrast to the TWI thresholds calculated for Dar and Addis which were calibrated based on calculated inundation profiles, the threshold value for Ouaga is calibrated based on the inundation area of the 2009 flooding event (Figure 33).

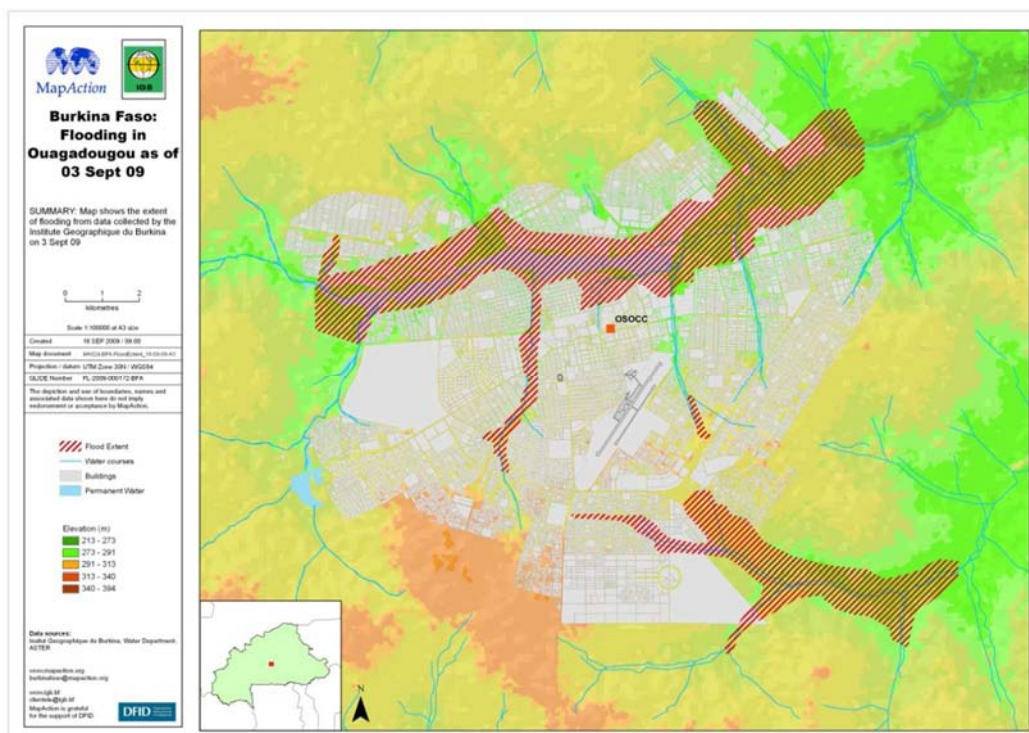


Figure 34 - Inundation profile of the event append in Sep 09

Based on the information available at the internet site (<http://www.mapaction.org/map-catalogue/mapdetail/1719.html>), it was possible to geo-reference the previous image and generate a spatial dataset.

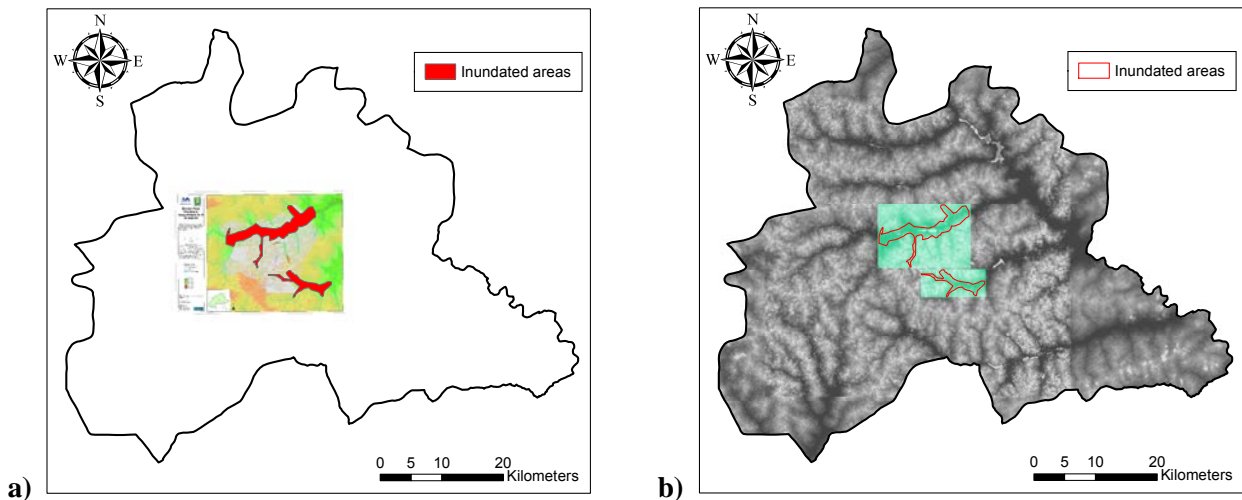


Figure 35 - a) Inundation areas after the 2009 events, b) Area 1 (the smaller) and Area 2 (the bigger)

Two areas are identified, one bigger than the other. In the follow the small area is called Area 1 and the big area is called Area 2.

3.3.3 Maximum likelihood estimation of the flood-prone threshold

In this section, it is demonstrated how the procedure described previously in Section 2.2 can be applied in order to calculate the likelihood of being flood prone as a function of the TWI threshold. In this case, the Bayesian parameter estimation is adopted based on information from more than one spatial window (Section 2.2.1). In particular, the information acquired from the study of the Area 1 are used as a-priori information for the study of the Area 2.

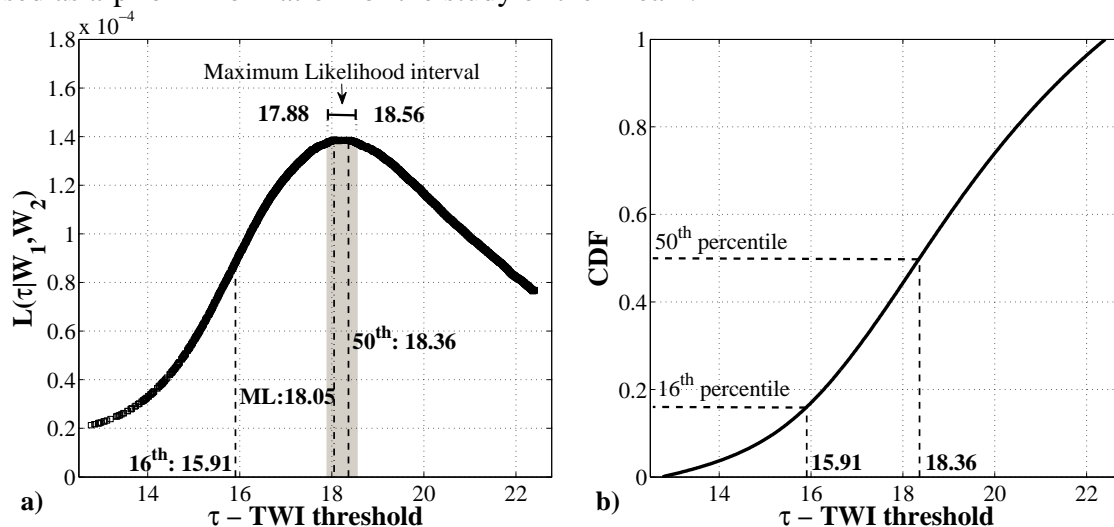


Figure 36 - The likelihood function $L(\tau|W_1, W_2)$, b) threshold CDF

Table 7 reports the threshold values that are calculated with the proposed procedure.

τ_{ML}	τ_{16}	τ_{50}	τ_{ML}^-	τ_{ML}^+
18.05	15.91	18.36	17.88	18.56

Table 7 - The statistics for the TWI threshold distribution for the case of Ouagadougou

It is possible to observe in Figure 37a that the TWI map with a threshold equal to the maximum likelihood TWI threshold τ_{ML} matches the spatial extent of the areas inundated by the 2009 flooding event. Moreover, the corresponding map of the flood-prone area for the entire city of Ouagadougou is shown in Figure 37b.

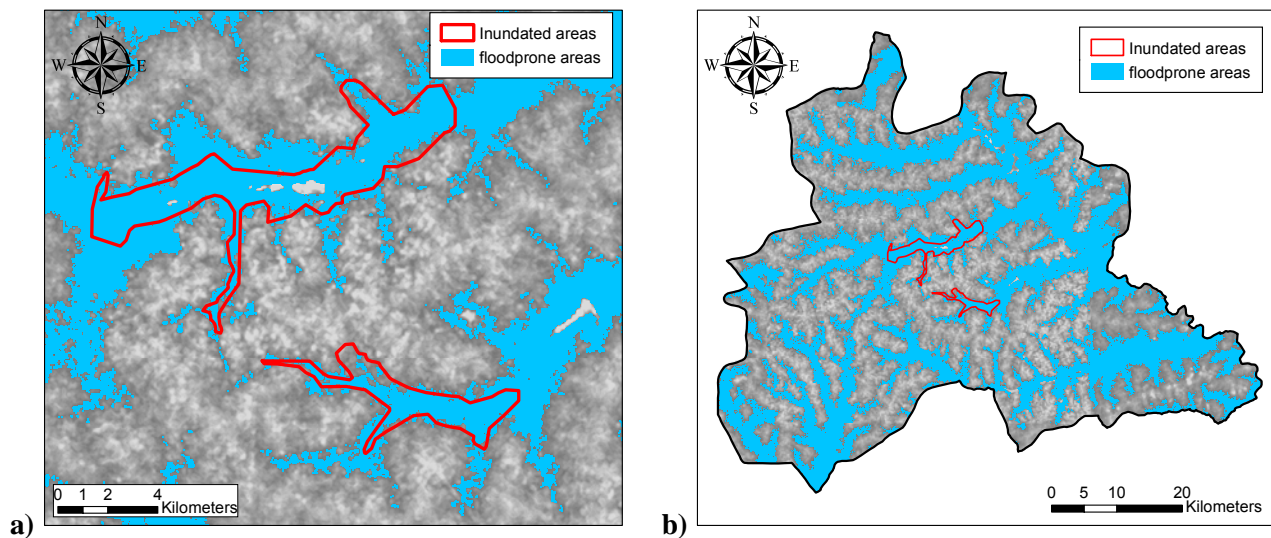


Figure 37 -999 a) Matching for the inundate areas, b) flood prone areas for the entire city

CONCLUSIONS

Urban hot spots for residential buildings and urban corridors (major roads) are delineated by overlaying two GIS-based datasets, namely, the topographic wetness index (TWI) and the urban morphology types (UMT). The flood prone areas based on the TWI method are identified by delineating the areas distinguished with TWI larger than a certain threshold. This threshold can be calibrated based on available information, such as inundation profiles calculated for a certain area within the basin. A probabilistic GIS-based method is used for calculating the maximum likelihood estimate and the 16th and 50th percentiles for the TWI threshold based on available inundation profiles. Bayesian parameter estimation is used to evaluate the threshold based on inundation profiles calculated for more than one area within the basin. The flood prone areas delineated for various threshold statistics (e.g. ML, 16th percentile) are then overlaid with the UMT units identified as residential and urban corridors in order to identify the urban hot spots and the areal extent of the UMT units affected by flooding. Integrating the population density as a geo-spatial dataset, leads to estimation of the number of people affected by flooding.

This methodology is applied to delineate the urban hotspots for flooding for the two case-study cities of Addis Ababa, Dar es Salaam and Ouagadougou. The resulting likelihood function for the TWI threshold sometimes reveals an interval in which it reaches its maximum value and remains more-or-less invariable --coined as the 99% maximum likelihood interval. The maximum likelihood estimate seems to be not particularly sensitive to the return period corresponding to the inundation profile. Incorporating the inundation profiles calculated for two different zones seems not to affect the maximum likelihood estimate significantly, although it leads to wider 99% maximum likelihood intervals. Differences in exposure characteristics have been assessed for a range of different residential types.

Addis Ababa: In particular, it can be observed that the mud and wood category constitutes around 50% of the residential buildings that are located in the flood prone areas in Addis Ababa. Moreover, the inhabitants of the mud and wood buildings are estimated to be around 67% of the people living in the flood prone areas. It is estimated that between around 3.6% (50th percentile) to 24% (16th percentile) of the total population of Addis may be affected by flooding. Between 3.4% (50th percentile) and 24.4% (16th percentile) of the total area of major urban roads is estimated to be affected by flooding.

Dar Es Salaam: It can be observed that the two categories mixed and scattered settlements together constitutes around 80% of the residential buildings that are located in the flood prone areas in Dar es Salaam. These two building categories together host around 80% of the population affected by flooding. It is estimated that between around 6.5% (50th percentile) to 38% (16th percentile) of the total population of Dar es Salaam may be affected by flooding. Between 4% (50th percentile) and 30% (16th percentile) of the total area of major urban roads is estimated to be affected by flooding.

Ouagadougou: The map of flood-prone areas for the whole city is calibrated based on the actual flooding extent as a result of the 2009 flooding event. Bayesian updating is employed in order to incorporate the information on the two observed flood-prone areas.



It is important to emphasize that considering the uncertainty in the TWI threshold leads to considerable difference in the estimated exposure to flooding. This highlights the importance of taking into account the various sources of uncertainty in the delineation of urban hot spots to flooding. The probabilistic methodology presented in this report can be used also to estimate the TWI threshold based on maps of flood prone areas based on previous flooding events.

How this methodology can be useful to urban planners?

Once this procedure is developed as a software, it can be used by urban planners to develop their own maps of the urban hotspots. The maps obtained based on the proposed procedure provide a quick screening tool to the urban planner in order to individuate efficiently the zones that need his/her immediate or long-term actions. These actions can include for example adoption of more accurate small-scale risk assessment procedures and undertaking various prevention strategies. The prevention strategies range from planning for structures that help in mitigating the flood risk, to relocation policies (if advisable), territory restriction measures and actions that aim at increasing of public awareness.



REFERENCES

Apel, H., Aronica, G.T., Kreibich, H., Thielen, A.H. (2009). “Flood risk analyses—how detailed do we need to be?”. *Nat. Hazard*, 49:79–98.

Cavan, G., Lindley, S., Yeshitela, K., Nebebe, A., Woldegerima, T., Shemdoe, R., Kibassa, D., Pauleit, S., Renner, R., Printz, A., Buchta, K., Coly, A., Sall, F., Ndour, N. M., Ouédraogo, Y., Samari, B. S., Sankara, B. T., Feumba, R. A., Ngapgue, J. N., Ngoumo, M. T., Tsalefac, M., Tonye, E. (2012) Green infrastructure maps for selected case studies and a report with an urban green infrastructure mapping methodology adapted to African cities CLUVA project deliverable D2.7. Available at http://www.cluva.eu/deliverables/CLUVA_D2.7.pdf. Date last accessed, Dec. 18th 2012.

FLO-2D Software, Inc, 2004. FLO-2D® User’s Manual, Nutrioso, Arizona, www.flo-2.com.

Gill, S.E., Handley, J.F., Ennos, A.R. Pauleit, S., Theuray, N., and Lindley, S.J. (2008). “Characterising the urban environment of UK cities and towns: a template for landscape planning in a changing climate”. *Landscape and Urban Planning* 87: 210–222.

HEC-RAS 4.1 (2010). Hydrological Engineering Center (HEC) River Analysis System (RAS). United States Army Corps of Engineering (USACE), www.hec.usace.army.mil

Jaynes, E.T. (1995). “Probability Theory: The logic of science”. Book.

Kirby, M. J. (1975). “Hydrograph modelling strategies”. *Progress in physical and human geography*, R. F. Peel, M. D. Chisholm, and P. Haggett, eds., Heinemann, London, 69-90.

Manfreda, S., Sole, A., and Fiorentino, M. (2007). “Valutazione del pericolo di allagamento sul territorio nazionale mediante un approccio di tipo geomorfologico.” *L’Acqua*, 4, 43-54 (in Italian).

Manfreda, S., Sole, A., and Fiorentino, M. (2008). “Can the basin morphology alone provide an insight on floodplain delineation?” *On flood recovery innovation and response*, WIT, Southampton, UK, 47-56.

Manfreda, S., Di Leo, M., Sole, A. (2011). “Detection of Flood-Prone Areas Using Digital Elevation Models.” *Journal of Hydrologic Engineering*, Vol. 16, No. 10, ASCE, 781-790

Nyarirangwe, M. (2008). The impact of multi-nucleated city morphology on transport in Addis Ababa (2008) in van Dijk, M. P. and Fransen, J Managing Ethiopian cities in an era of rapid urbanization. Eburon Uitgeverij BV.

Qin, Z.c., Zhu, A.X., Pei, T., Li, B.L., Scholten, T., Behrens, T., Zhou, C.H. (2011). “An approach to computing topographic wetness index based on maximum downslope gradient”. *Precision Agric*, 12:32–43.

Pauleit, S. and Duhme, F. (2000). “Assessing the environmental performance of land cover types for urban planning”. *Landscape and Urban Planning*, 52 (1): 1-20.